Grain size and transport biases in an Ediacaran detrital zircon record

Marjorie D. Cantine[1], Jacob B Setera[2], Jill A VanTongeren[2], Chiza Mwinde[3], and Kristin D Bergmann[1]

[1]Massachusetts Institute of Technology
[2]Rutgers University
[3]University of Chicago

November 21, 2022

Abstract

Detrital zircon records of provenance are used to reconstruct paleogeography, sediment sources, and tectonic configuration. Recognition of the biases in detrital zircon records that result from hydraulic sorting of sediment and the initial characteristics of zircons in source regions (e.g., size and abundance) has added new complexity and caution in the interpretation of these records. In this study, we examine the role of transport process and sediment sorting in these records. We begin our analysis by investigating the influence of grain size and transport process in biasing detrital zircon provenance records in an idealized sedimentary system. Our modeling results show that settling and selective entrainment can leave distinct, process-dependent fingerprints in detrital zircon spectra if initial size variation between source zircon populations exists. We then consider a case study: a detrital zircon record from Ediacaran to Terreneuvian Death Valley. We focus on the Rainstorm Member, which is geochemically, mineralogically, and sedimentologically unusual. In addition to Earth's largest negative carbon isotope excursion (the Shuram excursion), the Rainstorm Member also contains anachronistic carbonate structures and a detrital mineral suite enriched in heavy minerals. We evaluate the detrital zircon provenance record of the Rainstorm Member, and find that, despite its unusual character, the provenance of the unit is similar to other units in the succession, with substantial input from Yavapai-Matzatzal provinces. Size and density measurements of heavy and light density components of the deposit suggest that its enriched heavy mineral suite is best explained through concentration by selective entrainment and winnowing. We find that our detrital zircon dataset is susceptible to hydrodynamic fractionation, so that grain size exerts influence on its provenance record, in particular for large Grenville-aged (1.0-1.2 Ga) grains.

Grain size and transport biases in an Ediacaran detrital zircon record

Marjorie D. Cantine[1], Jacob B. Setera[2,3], Jill A. VanTongeren[2,4], Chiza Mwinde[5], Kristin D. Bergmann[1]

[1]Department of Earth, Atmospheric and Planetary Science, Massachusetts Institute of Technology, 77 Massachusetts Avenue, Cambridge, MA 02139
[2]Department of Earth and Planetary Sciences, Rutgers University, Busch Campus, 610 Taylor Rd., Piscataway, NJ 08854
[3]current institution: Department of Earth and Atmospheric Sciences, Cornell University, 112 Hollister Drive, Ithaca NY, 14853
[4]current institution: Department of Earth and Ocean Sciences, Tufts University, Lane Hall, Medford MA, 02155
[5]Department of the Geophysical Sciences, University of Chicago, 5734 S. Ellis Avenue, Chicago, IL 60637

ABSTRACT

Detrital zircon records of provenance are used to reconstruct paleogeography, sediment sources, and tectonic configuration. Recognition of the biases in detrital zircon records that result from hydraulic sorting of sediment and the initial characteristics of zircons in source regions (e.g., size and abundance) has added new complexity and caution in the interpretation of these records. In this study, we examine the role of transport process and sediment sorting in these records. We begin our analysis by investigating the influence of grain size and transport process in biasing detrital zircon provenance records in an idealized sedimentary system. Our modeling results show that settling and selective entrainment can leave distinct, process-dependent fingerprints in detrital zircon spectra if initial size variation between source zircon populations exists. We then consider a case study: a detrital zircon record from Ediacaran to Terreneuvian Death Valley. We focus on the Rainstorm Member, which is geochemically, mineralogically, and sedimentologically unusual. In addition to Earth's largest negative carbon isotope excursion (the Shuram excursion), the Rainstorm Member also contains anachronistic carbonate structures and a detrital mineral suite enriched in heavy minerals. We evaluate the detrital zircon provenance record of the Rainstorm Member, and find that, despite its unusual character, the provenance of the unit is similar to other units in the succession, with substantial input from Yavapai-Matzatzal provinces. Size and density measurements of heavy and light density components of the deposit suggest that its enriched heavy mineral suite is best explained through concentration by selective entrainment and winnowing. We find that our detrital zircon dataset is susceptible to hydrodynamic fractionation, so that grain size exerts influence on its provenance record, in particular for large Grenville-aged (1.0-1.2 Ga) grains.

INTRODUCTION

Zircon's durability and utility as a geochonometer make it a valuable tool in provenance studies. After zircon grains are eroded, transported, and redeposited, an interpretation of their original source regions can be made by matching their measured U/Pb ages to source regions of known age. High-throughput dating by laser ablation has enabled a rich literature in which detrital zircon grains constrain paleogeography, sediment provenance, and tectonics (e.g., (Stevens et al., 2010; Cawood et al., 2012, 2013; Mackey et al., 2012; Gehrels, 2014; Blum et al., 2017). Fundamental to the use of detrital zircon as a provenance tracer is the assumption that, to some substantial degree, the detrital zircon grains analyzed within a sample are representative of the rest of the bulk sediment. However, geological phenomena may lead to dissimilarities between the detrital zircon population and bulk sediment of a sample.

Zircon is a robust mineral (Smithson, 1950; Carroll, 1953; Morton and Hallsworth, 2007). This hardiness allows zircon grains to survive not only transport over long distances, but also multiple sedimentary cycles of erosion, transport, and deposition (Fedo et al., 2003; Hawkesworth et al., 2009). This recalcitrance can lead to difficulty in interpreting the record of provenance captured by detrital zircons: the measured ages of zircon grains may correspond either with igneous or metamorphic terranes actively eroded at the time of deposition of the sediment (primary cycle grains) or during previous sedimentary cycles (polycyclic grains). Careful analysis of grain cores and rims and comparison with other minerals can reveal the polycyclic character of some zircons (Hietpas et al., 2011a; Flowerdew et al., 2019; Moecher et al., 2019).

Other deviations can arise from source area variation in zircon fertility, which can span several orders of magnitude even over regional spatial scales (Dickinson, 2008; Malusà et al., 2016). Zircon-rich and zircon-poor terranes are not represented in the detrital zircon record in proportion to the bulk sediment they contribute, but in proportion to their zircon fertility (Moecher and Samson, 2006; Dickinson, 2008; Hietpas et al., 2011b; Malusà et al., 2016; Spencer et al., 2018; Chew et al., 2020; Guo et al., 2020). In Laurentia, the Mesoproterozoic Grenville province (1.0-1.2 Ga) is particularly zircon-rich (Moecher and Samson, 2006; Samson et al., 2018); these and other igneous rocks associated with the assembly of Rodinia have high Zr concentrations (Liu et al., 2017).

The co-variation of detrital zircon age, or source region, and grain size is the source of deviation most relevant to the present study. Some evidence suggests that, in general, older zircons are finer and less variable in size than younger grains (Lawrence et al., 2011; Yang et al., 2012), although not all studies support this conclusion (Muhlbauer et al., 2017). Terrane-specific size differences may exist, too. In Laurentia, Grenville sources may produce large (long axis on the order of 1000 μm) zircons (Moecher and Samson, 2006; Samson et al., 2018). By comparison, the nearby Neoproterozoic Carolina terrane produces much smaller (50 micron long axis) zircons. These smaller zircons are, volumetrically, hundreds to thousands of times smaller than the *tips* of large Grenville zircons (Moecher and Samson, 2006, see their Fig. 5).

If detrital zircons from a particular source region are characteristically large or small, then sediment sorting will systematically emphasize or deemphasize the apparent contribution of that source, independent of sediment provenance. Studies of some modern (Hietpas et al., 2011b; Lawrence et al., 2011; Slama and Kosler, 2012; Ibañez-Mejia et al., 2018; Malkowski et al., 2019) and ancient systems (Augustsson et al., 2017, 2019) show that grain size does exert control on some records of provenance. Studies of modern sediments even capture statistically significant variation in detrital zircon provenance over a single sand dune (Lawrence et al., 2011) or river profile (Ibañez-Mejia et al., 2018) due to hydrodynamic sorting of sediment, despite these samples' common transport history and provenance. In other successions, grain size does not appear to be a major control on detrital zircon records of provenance (Muhlbauer et al., 2017; Leary et al., 2020).

Analytical procedures may enhance some size-dependent effects. Selection of large grains (>100 μm) for analysis biases selection for coarse-grained granitoid sources (Gehrels, 2000). Mineral separation and hand-picking of grains may contribute additional size-dependent analytical bias that minimizes the impact of smaller grains (Gehrels, 2000; Moecher and Samson, 2006; Slama and Kosler, 2012). In studies of Laurentia, Grenville-aged sources are reported to have particularly large zircon grains that may be systematically selected for analysis (Moecher and Samson, 2006; Samson et al., 2018), contributing analytical bias to geological exaggeration of this fertile source region in provenance records. Analysis of a consistent size class (63-125 μm) is suggested as a strategy to mitigate the effects of hydrodynamic fractionation (Morton and Hallsworth, 1994; Morton et al., 1996). However, this strategy enhances, rather than minimizes, size-dependent effects (Garzanti et al., 2009) because this narrow size window will contain heavy mineral grains for one bulk sediment size, but light mineral grains for a finer sediment. The current best practice to mitigate these size-dependent biases is to measure both grain size and grain age and determine what, if any, relationship exists between these variables (Malusà and Garzanti, 2019).

In this study, we explore how sedimentary size sorting, as well as size-density relationships induced by transport process, may affect detrital zircon provenance records. First, we use size-density relationships from both meta-analyses of settling experiments (Dietrich, 1982; Bagheri and Bonadonna, 2016; Raffaele et al., 2020) and observations of natural sands (Hand, 1967; Steidtmann and Haywood, 1982; Garzanti et al., 2008) to model the process-dependent depositional size difference between the light mineral quartz (density or $\rho = 2.65$ g/cm^3) and the heavy mineral zircon, ($\rho = 4.65$ g/cm^3) in an idealized sedimentary system. We apply these insights to investigate the role of grain size in shaping a detrital zircon record from an Ediacaran to

Terreneuvian sedimentary succession from Death Valley, Nevada and California, USA. This succession includes the Rainstorm Member of the Johnnie Formation, a unit that is sedimentologically, mineralogically, and geochemically anomalous. We leverage insights from our analysis of grain size and provenance to further constrain the depositional setting and transport mechanisms related to Rainstorm Member's peculiar deposits.

Size-Density Relationships in Clastic Deposits

Grains with the same uniform settling velocity are hydraulically equivalent and will be deposited together (Rubey, 1933). The settling velocity of a particle is a function of its size, shape, roundness, and density, as well as of the properties of the fluid through which it settles. Grain size and density are the most important variables in determining settling velocity for subspherical grains (Dietrich, 1982), and increases in grain density are compensated by decreases in grain diameter. For this reason, zircon (ρ = 4.65 g/cm^3) grains are typically deposited with larger quartz (ρ = 2.65 g/cm^3) grains.

Empirical relationships derived from meta-analyses of settling experiments that span a wide range of grain sizes, densities, shapes, and fluid properties (e.g., Clift and Gauvin, 1971; Gibbs et al., 1971; Dietrich, 1982; Cheng, 1997; Ferguson and Church, 2004; Bagheri and Bonadonna, 2016; Raffaele et al., 2020) capture the combined effects of turbulence and fluid viscosity on settling velocity. **Figure 1** illustrates empirically derived relationships between grain size and settling velocity for quartz and zircon in both water (using the relationship defined by Dietrich, 1982; assuming a Corey Shape Factor of 0.7 and a Powers roundness value of 3.5, typical values for natural sediments) and air (using the equation of Bagheri and Bonadonna, 2016; with coefficients from Raffaele et al., 2020). These relationships predict that, relative to a constant quartz grain size, zircon grains deposited in air will be larger than zircon grains deposited in water. This difference is driven by the greater contrast between the submerged density of quartz and zircon grains in water compared to air, and is observed in some natural sands (e.g., McIntyre, 1959; Friedman, 1961; Steidtmann and Haywood, 1982).

However, many natural sediments exhibit size-density relationships inconsistent with these predictions. Garzanti et al. (2008) find that, within aeolian and beach sands sourced from the modern Po River delta, aeolian heavy mineral grains are smaller than beach heavy mineral grains relative to the quartz sediment in each. In beach and aeolian sands from New Jersey, Hand (1967) observes heavy minerals that are smaller than predicted by settling relationships. Steidtmann and

Haywood (1982) compare tourmaline and quartz grains within the aeolian Casper Formation, and find that although grainfall laminae have size-density relationships consistent with settling through air, grains from subcritical climbing ripples have size-density relationships in which tourmaline grains are much smaller than predicted. Size-density relationships that deviate from equal settling velocity, in which heavy minerals are smaller than predicted, are also found in other natural sediments (Rittenhouse, 1943; McIntyre, 1959; Briggs, 1965; Grigg and Rathbun, 1965; Lowright et al., 1972; Slingerland, 1977; Komar and Wang, 1984).

Various processes operating during sediment transport can lead to size-density relationships other than that predicted by settling velocity (Lowright et al., 1972; Slingerland, 1977, 1984; Komar and Wang, 1984; Slingerland and Smith, 1986; Komar et al., 1989; Komar, 2007). Larger grains resting on a bed project further into the profile of the flow above them and have a smaller pivot angle than smaller grains. This encourages selective entrainment of larger, lighter grains rather than smaller, denser grains (McIntyre, 1959; Lowright et al., 1972; Slingerland, 1977, 1984; Komar and Li, 1988; Komar et al., 1989). Shear sorting during transport leads density-stratified deposits in which dispersive equivalence, rather than entrainment or settling velocity, controls the size-density distribution of deposits (Emery and Stevenson, 1950; Clifton, 1969; Sallenger, 1979). Variations in flow over bedforms like ripples and dunes can lead to preferential deposition of heavy minerals near the crest of bedforms (McQuivey and Keefer, 1969; Brady et al., 1973). Localized, preferential deposition of heavy minerals can also occur in response to flow changes around larger geomorphic features like bars or river confluences (Smith and Beukes, 1983; Day and Fletcher, 1989).

We consider two end-member possibilities related to selective entrainment in our study of detrital zircon provenance records. At one extreme, detrital zircon grains within a deposit are as large as quartz grains. In this case, size and pivot angle control entrainment more strongly than grain density; coarse light grains are selectively entrained; and the deposit becomes heavy mineral-enriched and well-sorted, as observed in some placer deposits (Slingerland, 1977). At the other extreme, detrital zircon grains are much smaller than predicted by settling, a relationship observed in many natural sands (Rittenhouse, 1943; McIntyre, 1959; Briggs, 1965; Grigg and Rathbun, 1965; Hand, 1967; Lowright et al., 1972; Slingerland, 1977; Steidtmann and Haywood, 1982; Komar and Wang, 1984; Komar, 2007; Garzanti et al., 2008). This scenario is thought to arise due to the shielding of small heavy minerals by larger, lighter grains, leading to a difference in settling velocity but equivalence in entrainment potential between larger light grains and smaller dense grains (Hand, 1967; Steidtmann and Haywood, 1982; Komar and Wang, 1984; Komar and Li, 1988; Komar, 2007). Both extremes are the result of complex interactions between grain size and shape, bed roughness, and fluid flow during transport near the bed. Size-density relationships for sediments deposited by settling are intermediate between these two extremes. We hypothesize that, for sediments in which detrital zircon populations exhibit significant size differences between source areas, transport processes may impart different, size-dependent biases in their provenance record even if bulk sediment size is constant.

GEOLOGICAL CONTEXT

We now consider the role of grain size in shaping a specific detrital zircon record. The Johnnie Formation, Stirling Quartzite, and Wood Canyon Formation are Ediacaran to Terreneuvian units within the mixed siliciclastic-carbonate, rift-to-passive margin succession of Death Valley, USA, which thickens westward (**Figure 2**) (Stewart, 1970; Summa, 1993; Fedo and Cooper, 2001; Corsetti and Kaufman, 2003; Clapham and Corsetti, 2005; Verdel et al., 2011; Schoenborn et al., 2012). The underlying Noonday Dolomite is correlated with post-Marinoan cap carbonate units (Prave, 1999; Halverson et al., 2005; Petterson et al., 2011), especially those also containing tubestone (Cloud et al., 1969; Hegenberger, 1987; Hoffman and Schrag, 2002; Hoffman et al., 2002; Rodrigues Nogueira et al., 2003; Corsetti and Grotzinger, 2005; Bold et al., 2016), so is interpreted as earliest Ediacaran in age at its base (Prave, 1999; Petterson et al., 2011; Creveling et al., 2016). The Wood Canyon Formation spans the Ediacaran-Cambrian boundary and contains Ediacaran fossils in its lower member (Diehl, 1979; Corsetti and Hagadorn, 2000; Hagadorn and Waggoner, 2000; Smith et al., 2017). Direct radiometric age constraints within the succession are limited; a detrital zircon dated to 640.33 ± 0.09 from the Johnnie Formation is consistent with an Ediacaran age for the unit (Verdel et al., 2011). Correlation of a carbon isotope excursion in the Rainstorm Member, the uppermost unit of the Johnnie Formation, with dated intervals in northwest Canada and Oman suggest that deposition of this unit took place after 574 ± 4.7 Ma (Rooney et al., 2020).

These units record the development of the Laurentian passive margin including some evidence for extensional tectonics (Stewart and Poole, 1974; Summa, 1993; Fedo and Cooper, 2001; Clapham and Corsetti, 2005). Braided channel facies and marine reworking of fluvial sand are common in the Johnnie Formation, along with intertidal to shallow subtidal carbonates containing stromatolites and ooids (Summa, 1993). Desiccation cracks, tepee structures, caliche, and karst surfaces throughout the shallow environments of the Johnnie Formation provide evidence for frequent, and sometimes long-lasting, exposure (Summa, 1993). Basinal environments in the lower Johnnie Formation record a submarine channel complex with no evidence for exposure (Williams et al., 1974; Troxel et al., 1982; Wright et al., 1984; Prave, 1999; Petterson et al., 2011; Macdonald et al., 2013a; Creveling et al., 2016) The Stirling Quartzite abruptly overlies the Johnnie Formation and is dominated by braided fluvial quartzite, though its middle member includes interbedded intertidal shale, dolomite, and siltstone (Stewart, 1970; Fedo and Cooper, 2001). Siltstone, locally arkosic quartzite, and minor carbonate make up the lower and upper members of the Wood Canyon Formation (Stewart, 1970). These units record deposition in shallow marine settings; its middle member, a locally conglomeratic, feldspathic quartzite, was deposited in a braided fluvial system (Stewart, 1970; Fedo and Cooper, 1990, 2001; Corsetti and Hagadorn, 2000; Hogan et al., 2011; Muhlbauer et al., 2017, 2020). Detrital zircon provenance records through this succession show varying contributions from the Grenville, Yavapai-Matzatzal, and mid-continent regions, and a smaller contribution from Archean sources, with the vast majority of zircons older than 1 Ga (Stewart et al., 2001; Verdel et al., 2011; Schoenborn et al., 2012; Muhlbauer et al., 2017). The Wood Canyon Formation features a sharp peak associated with Grenville-aged sources (Stewart et al., 2001; Muhlbauer et al., 2017).

The Rainstorm Member

The Johnnie Formation is subdivided into six members recognized by Stewart (1970). The uppermost of these, the Rainstorm Member, is a shallow marine, storm-dominated, mixed siliciclastic-carbonate unit with unusual sedimentological, mineralogical, and geochemical features (Stewart, 1970; Summa, 1993; Corsetti and Kaufman, 2003; Corsetti et al., 2004; Kaufman et al., 2007; Pruss et al., 2008; Bergmann et al., 2011, 2013). The detrital zircon and heavy mineral record of the Rainstorm Member, and what it reveals about provenance and process during deposition of this peculiar unit, is the focus of this study. The provenance of the Rainstorm Member is also investigated by Schoenborn et al. (2012). That study uses Nd isotopes in carbonate to constrain the provenance of the Rainstorm Member and suggests that the source of sediment is primarily the Yavapai-Matzatzal provinces. However, Schoenborn et al. (2012) note these data do not definitively distinguish between this scenario and one in which the sources include the Mojave and/or Yavapai-Matzatzal provinces and the Grenville province.

The regionally extensive Johnnie Oolite is a 2 m-thick, cross-stratified oolite bed near the base of the Rainstorm Member, and is bounded above and below by siltstone and shale (Stewart, 1970; Summa, 1993). Summa (1993) suggests a cryptic unconformity beneath the Johnnie Oolite. Above the Johnnie Oolite, siltstone and sandstone are interbedded with pink and gray limestone containing ooid grainstone, intraclast and edgewise conglomerate, and, locally, crystal fans (Stewart, 1970; Summa, 1993; Corsetti et al., 2004; Pruss et al., 2008; Bergmann et al., 2013). The siltstone and carbonate strata of the Rainstorm Member have been interpreted as a deposit associated with highstand and maximum flooding; initial marine transgression is recorded by the time-transgressive Johnnie Oolite (Summa, 1993; Bergmann et al., 2011). Hummocky cross-stratification, amalgamated scours, and planar lamination are abundant throughout the Rainstorm Member (Summa, 1993). Above these units, an incision surface cuts into the Rainstorm Member, in some locations eroding it completely; these incised valleys are filled by thick conglomerate and may represent either subaerial or submarine erosion (Stewart, 1970; Summa, 1993; Corsetti and Kaufman, 2003; Clapham and Corsetti, 2005; Trower and Grotzinger, 2010; Verdel et al., 2011). This incision surface is interpreted either as tectonic (Summa, 1993; Clapham and Corsetti, 2005) or glacioeustatic (Christie-Blick and Levy, 1989; Abolins et al., 2000; Witkosky and Wernicke, 2018) in origin.

Pink-gray Rainstorm carbonate units are the only limestone strata in the Johnnie Formation; other carbonate is dolostone (Summa, 1993). In the Southern Nopah range, Rainstorm limestone beds also contain carbonate crystal fans neomorphosed to calcite from primary aragonite (Summa, 1993; Corsetti et al., 2004; Pruss et al., 2008; Bergmann et al., 2013) (**Figure 3**). These delicate crystal fans grew from the seafloor, nucleating on horizons of detrital, iron-rich material (Summa, 1993; Pruss et al., 2008; Bergmann et al., 2013). These nucleation surfaces contain a striking diversity of minerals, including calcite, dolomite, quartz, hematite, rutile, anatase, ilmenite, muscovite, biotite, apatite, barite, monazite, and zircon (Bergmann et al., 2013). Crystal fans are about a centimeter in height and individual blades have a horizontal hexagonal cross section with a maximum diameter of 230 μm (Pruss et al., 2008). Sediment between crystal blades includes ooids, detrital mineral grains, and intraclasts (Pruss et al., 2008; Bergmann et al., 2013) (**Figure 3**).

Crystal fans like these are more typically associated with Archean or Paleoproterozoic successions and Mesoproterozoic peritidal environments (Grotzinger and Read, 1983; Hofmann and Jackson, 1987; Kah and Grotzinger, 1992; Kah and Knoll, 1996; Sumner and Grotzinger, 1996; Grotzinger and James, 2000; Allwood et al., 2009; Higgins et al., 2009; Bergmann et al., 2013; Cantine et al., 2020). Where crystal fans occur in Neoproterozoic sediments, they are typically associated with cap carbonate units (Grotzinger and James, 2000; Sumner and Grotzinger, 2000; James et al., 2001; Hoffman and Schrag, 2002; Babinski et al., 2007; MacDonald et al., 2009) and not with middle Ediacaran strata. Rainstorm crystal fans are thus anachronistic.

Yet like other examples of crystal fans through Earth history (Bergmann et al., 2013), Rainstorm crystal fans are interpreted to have developed during a period of maximum flooding and low background sedimentation rate (Summa, 1993; Corsetti et al., 2004; Pruss et al., 2008; Bergmann et al., 2013) The formation of Rainstorm crystal fans may be linked to minimal organic delivery and limited aerobic respiration maintaining favorable conditions for carbonate growth at the sediment-water interface (Bergmann et al., 2013). Most Rainstorm crystal fan layers remain *in situ*, and the small size and delicate shape of the crystal fans suggests that they formed in relatively quiet conditions (Summa, 1993; Pruss et al., 2008). Crystal fan intraclasts (Bergmann et al., 2013, their figure 5) show that some crystal fan-bearing units were disrupted and reworked during high-energy events.

In addition to crystal fans, the Rainstorm Member's pink and gray limestone hosts the nadir of an extremely negative carbon isotope excursion, which contains values as low as -12‰ $\delta^{13}C$; the onset of the excursion is within the Johnnie Oolite (Corsetti and Kaufman, 2003; Kaufman et al., 2007; Bergmann et al., 2011; Verdel et al., 2011). The asymmetric excursion is characterized by a rapid onset and gradual recovery (Corsetti and Kaufman, 2003; Kaufman et al., 2007; Bergmann et al., 2011; Verdel et al., 2011). The excursion is synchronous across the Death Valley area (Bergmann et al., 2011; Minguez et al., 2015). An estimate for the duration of the Rainstorm excursion, derived from magnetostratigraphic constraints and extrapolation of sedimentation rate, yields 8.2 ± 1.2 million years (Minguez et al., 2015). Another independent estimate derived from subsidence modeling yields a duration of c. 6 million years (Witkosky and Wernicke, 2018).

The Rainstorm excursion is putatively correlated with Earth's most negative carbon isotope excursion, the Shuram excursion (Corsetti and Kaufman, 2003; Kaufman et al., 2007; Bergmann et al., 2011; Grotzinger et al., 2011; Verdel et al., 2011; Minguez et al., 2015; Witkosky and Wernicke, 2018). The Shuram excursion is observed on multiple continents in middle Ediacaran strata. It is consistently characterized by a rapid onset to strongly negative $\delta^{13}C$ values followed by gradual recovery (e.g., Burns and Matter, 1993; Fike et al., 2006; KauFormationan et al., 2006; Le Guerroué et al., 2006c; Bowring et al., 2007; Zhu et al., 2007; Jiang et al., 2007; Melezhik et al., 2008; Le Guerroué, 2010; Macdonald et al., 2013b; Husson et al., 2015; Canfield et al., 2020). Recent geochronological work indicates the Shuram excursion was a global and synchronous event with a duration of less than 6.7 ± 5.6 million years (Canfield et al., 2020; Matthews et al., 2020; Rooney et al., 2020). Because the Rainstorm excursion shares its magnitude; asymmetric onset and recovery; position within middle Ediacaran strata; and a similar duration with the Shuram excursion, like others (Corsetti and Kaufman, 2003; Kaufman et al., 2007; Bergmann et al., 2011; Grotzinger et al., 2011; Verdel et al., 2011; Minguez et al., 2015; Witkosky and Wernicke, 2018), we consider the Rainstorm excursion a regional expression of the global Shuram excursion and refer to the negative carbon isotope excursion within the Rainstorm Member as the Shuram excursion.

The magnitude and global extent of the Shuram excursion have made it a particular puzzle for geochemists and geobiologists. Geochemical questions revolve around the primary (Rothman et al., 2003; Fike et al., 2006; Bristow and Kennedy, 2008; McFadden et al., 2008; Ader et al., 2009; Bjerrum and Canfield, 2011; Johnston et al., 2012; Lee et al., 2015; Miyazaki et al., 2018; Shields et al., 2019) or post-depositional (Knauth and Kennedy, 2009; Derry, 2010; Schrag et al., 2013; Oehlert and Swart, 2014) processes capable of driving such a large and apparently synchronous global excursion globally. Determining the impact, if any, of the Shuram excursion on the diversification, extinction, and habitats of early metazoans is also a critical geobiological question (Macdonald et al., 2013b; Wood et al., 2015; Cui et al., 2017; Darroch et al., 2018; Muscente et al., 2018; Zhang et al., 2019; Li et al., 2020; Rooney et al., 2020). The relationship between the regional Gaskiers glaciation c. 580 Ma (Pu et al., 2016) and the Shuram excursion has also provoked interest (Xiao et al., 2016), although recent age constraints (Canfield et al., 2020; Matthews et al., 2020; Rooney et al., 2020) and the recognition of a possible Shuram excursion equivalent in clastic-hosted carbonates in Newfoundland (Canfield et al., 2020) suggest that the two events are temporally distinct.

Our understanding of the Shuram excursion globally relies on a sound sedimentological understanding of the sediments that record it locally. The Rainstorm Member contains anachronistic crystal fans and unusual detrital mineral assemblages, suggesting it records unusual environmental conditions. It also contains Earth's largest negative carbon isotope excursion, suggests a tantalizing interplay between the unit's unusual sedimentology and the processes driving the excursion.

MATERIALS AND METHODS

Grain mixing model

To explore the influence of process-based size-density relationship on detrital zircon records, we built a numerical model. The model generates synthetic quartz and zircon grains for two source regions with defined age and size characteristics (**Fig. 4**). Quartz grains of all sizes are generated; by contrast, zircon grains have a characteristic size distribution. No initial size-density relationship between quartz and zircon grain sizes exists in the source regions.

Each individual grain is randomly assigned an age and grain size based on defined parameters for its source region. Each grain is also assigned a 2σ age uncertainty of 5% of the grain's age, mirroring the uncertainty associated with laser ablation $^{206}Pb/^{207}Pb$ age measurements. The source regions are mixed in a defined ratio. From the combined pool, 100 grains of quartz and zircon are then randomly selected, representing the deposition of grains. For quartz grains, the probability of being deposited are determined according to a defined mean grain size and standard deviation representing the characteristics of the sedimentary deposit. The deposited zircon grains are determined by a size-density relationship between the defined grain size of quartz to deposit and the corresponding zircon size. The age spectrum of the resulting deposited zircon "sample" is determined. Synthetic spectra are generated this way 10,000 times.

The model considers four possible different size-density relationships between quartz and zircon. In one end-member relationship, the "equal sizes" scenario, the zircons deposited have the same size as the quartz grains deposited—the greater density of the zircon grains has no effect on the size of zircon grains deposited. This scenario is potentially applicable to well-sorted, heavy mineral-rich deposits like placer sands that form under specific flow and bed roughness conditions (Slingerland, 1977). The other end-member relationship, the "grain shielding" scenario, uses the size-density relationship reported by Garzanti et al. (2008) from a modern aeolian sand, which we interpret as the result of selective entrainment and grain shielding. Similar deposits, in which heavy mineral grains have lower settling velocities than the quartz with which they are deposited, are reported elsewhere (Hand, 1967; Steidtmann and Haywood, 1982). Intermediate to these end-members are the size-density relationships empirically determined for quartz and zircon settling in water (Dietrich, 1982) and air (Bagheri and Bonadonna, 2016; Raffaele et al., 2020). For each case, these size-density relationships are shown in **Fig. 4, column II.**

In all cases described here, the two source regions are mixed in a 1:1 ratio, and the zircon fertility, or ratio of quartz grains to zircon grains in each region, is held constant at 10:1, an illustrative value. Geological measurements of zircon fertility are smaller (Malusà et al., 2016). The parameters for all runs are shown in **Table 1**. See the Data Availability section for information on the code used for this analysis.

Base case

This case mixes two source regions that are identical in every regard, including the grain sizes of zircons, except for the ages associated with the source regions. Grains from Source 1 have a population age of 1000 Myr with a standard deviation of 50 Myr; Source 2 grains have a population age of 500 Myr with a standard deviation of 50 Myr. The sizes of quartz grains from both source regions are uniformly distributed between 0 and 300 μm. Zircon from both regions has a mean grain size of 150 μm with a standard deviation of 15 μm. The deposited quartz sediment has a mean grain size of 200 μm with a standard deviation of 15 μm.

Case 1

This case is identical to the base case, with the single change that zircons from Source 2 are smaller than zircons from Source 1. Source 2 zircons have a mean grain size of 100 μm with a standard deviation of 15 μm.

Case 2

This case explores behavior in finer-grained sediments than previous cases. In this case, both Source 1 and 2 quartz grains have a mean grain size of 80 μm with a standard deviation of 15 μm. Source 1 zircons have a mean grain size of 40 μm with a standard deviation of 10 μm; Source 2 zircons have a mean grain size of 30 μm with a standard deviation of 10 μm. Deposited quartz has a mean grain size of 55 μm with a standard deviation of 5 μm. All other parameters are unchanged from the base case.

Rainstorm sample characterization

Samples were collected in the southern Nopah Range, including a very fine-grained quartz sandstone below the Johnnie Oolite and crystal fan-bearing strata within the Rainstorm Member. Sample locations are available in the Supplement. Standard zircon separation procedures, including magnetic and heavy liquid separation, were used for the sandstone sample. The crystal fan-bearing samples were dissolved in 20% hydrochloric acid to remove carbonate. After dissolution, the insoluble residue followed standard zircon separation procedures. Prior to analysis, zircons were mounted, polished, and imaged by either cathodoluminescence or light microscope.

Geochronology

U-Pb ages of zircons were obtained via LA-ICP-MS using a Photon Machines 193 nm laser ablation system coupled to a Thermo iCapQc™ mass spectrometer at Rutgers University. Laser power was set at 50% power and a 10 Hz rep rate, resulting in a fluence of 4.25 J/cm^2 at the surface of the zircon. The laser spot size was 20 μm. This small spot size was used to minimize sample destruction during analysis, so that any potential young, concordant grains could be dated with high-resolution U/Pb thermal ionization mass spectrometry (TIMS). Ablated material was carried to the plasma via Helium gas at a total flow rate of 0.8 LPM. For each analysis, the iCapQc™ was set up to acquire data for ~220 sweeps with a 10 millisecond per isotope dwell time. Laser firing and ablation lasted for 30 seconds during each analysis while gas blanks were measured for approximately 20 seconds immediately prior to each zircon analysis using the same instrumental conditions (without firing the laser). Washout time between each analysis and the start of the next background was approximately 1 minute. Data processing was performed primarily using the Iolite software package with ^{206}Pb/^{207}Pb ages calculated using ISOPLOT (Ludwig, 2003). ^{206}Pb/^{207}Pb ages are used in order to make direct comparison to the results of Schoenborn et al. (2012). The use of ^{206}Pb/^{238}U ages rather than ^{206}Pb/^{238}U ages would yield the same conclusions.

The primary standard used was the zircon standard 91500, with an age of 1065 Ma (Fisher et al., 2014). 91500 was run 190 times, yielding a weighted mean ^{206}Pb/^{238}U age of 1061.7 ± 1.8 Ma (2σ; MSWD = 2.1) and a ^{207}Pb/^{206}Pb age of 1085.7 ± 8.6 Ma (2σ; MSWD = 1.1). 91500 was run after every 10-15 samples. The results from the 91500 standard were used to apply a final fractionation correction to the unknowns via a bracketing approach. The zircon standards Plesovice (published age: 337 Ma; Slama et al., 2008), R33 (419 Ma), and Mud Tank (732 Ma) were also run during the session and processed the same way as the unknowns (Fisher et al., 2014). The Plesovice standard was run a total of 161 times and yielded a weighted mean ^{206}Pb/^{238}U age of 337.80 ± 0.71 Ma (2σ; MSWD = 3.5) and a ^{207}Pb/^{206}Pb age of 341.9 ± 7.5 Ma (2σ; MSWD = 0.9). The R33 standard was run a total of 84 times and yielded a weighted mean ^{206}Pb/^{238}U age of 419.6 ± 1.8 Ma (2σ; MSWD = 7.4) and a ^{207}Pb/^{206}Pb age of 468 ± 18 Ma (2σ; MSWD = 1.2). The Mud

Tank standard was run a total of 55 times and yielded a weighted mean $^{206}Pb/^{238}U$ age of 724.1 ± 3.4 Ma (2σ; MSWD = 3.0) and a $^{207}Pb/^{206}Pb$ age of 737 ± 33 Ma (2σ; MSWD = 0.9).

Due to the small spot size used and low Pb signal, the uncertainty of individual $^{207}Pb/^{206}Pb$ ages is substantial, especially in the Phanerozoic secondary standards. However, our samples do not include Phanerozoic zircon grains and typically have significantly lower individual $^{207}Pb/^{206}Pb$ age uncertainties than those of the standards. The concordance of the Mesoproterozoic 91500 standard supports a good degree of confidence in the analyses; and our analysis focuses on distinct Proterozoic detrital zircon age subpopulations that are resolvable within the error achieved. Grains were screened for concordance between their $^{206}Pb/^{238}U$ and $^{207}Pb/^{206}Pb$ ages, and only those with ± 10% concordance were included in the analysis. Ages presented are $^{207}Pb/^{206}Pb$ ages.

Age data from the lower and middle Johnnie Formation and the Stirling Quartzite were previously published in Schoenborn et al. (2012). Age data from the upper Stirling Quartzite and Wood Canyon Formation were published in Muhlbauer et al. (2017).

Zircon size determination

The long and short axis of each grain from the Rainstorm Member was measured, either by cathodoluminescence (CL) imaging or light microscope. Cathodoluminescence images of grains from the lower and middle Johnnie Formation and lower and upper Stirling Quartzite (Schoenborn et al., 2012) are available in the appendices of (Schoenborn, 2010). Grain long axes for upper Stirling Quartzite and Wood Canyon Formation samples were previously published in Muhlbauer et al. (2017). Only concordant grains for which a grain size could be determined are included in this study.

Previous detrital zircon grain size studies have used either the equivalent spherical diameter (ESD) of zircon grains (e.g., Lawrence et al., 2011) or the long axis of grains (e.g., Muhlbauer et al., 2017). The ESD better accounts for the hydrodynamic characteristics of a zircon grain than a measurement of its long axis alone (Garzanti et al., 2008; Lawrence et al., 2011), however, data easily available for all grains was limited to measurements of long axes. This study uses the long axis of detrital zircons to quantify their grain size, though the size trends described in this study are consistent using ESD within the subpopulation of samples for which ESD can also be calculated.

Crystal fan size-density determination

A sample of crystal fan-bearing carbonate from the Rainstorm Member was dissolved as described above in 20% hydrochloric acid. The residue was rinsed with deionized water and dried. This sample did not undergo magnetic separation and was separated into a heavy and light fraction using the heavy liquid methylene iodide (ρ = 3.32 g/cm^3). The majority of the detritus, both by volume and by mass, separated into the heavy fraction (**Table 2**). The density of both fractions was determined through volume displacement with a 10 mL volumetric flask, sensitive balance, and deionized water. The grain sizes of the heavy and light fractions were determined using a laser particle size analyzer at the University of Oklahoma.

Modeling size-provenance relationships in the Ediacaran-Terreneuvian Death Valley succession

To explore the signature of grain size in data from this succession, we pooled all measured age and grain size data for zircon grains from these units. We defined 4 size distributions, each corresponding to the size distributions of zircon grains from a particular unit: 69 ± 16 μm (1 sd; Rainstorm crystal fans); 89 ± 21 μm (1 sd; Rainstorm sandstone); 124 ± 32 μm (1 sd; Lower Johnnie Formation) and 154 ± 50 μm (1 sd; Wood Canyon Formation). Then, these size distributions were used to randomly select 60 grains from the pool of all zircons, a process repeated 10,000 times. The resulting age spectra from each subset of 60 grains was determined. See the Data Availability section for information on the code used for this analysis.

RESULTS

Size mixing model

Results from our exploration of size-density relationships within detrital zircon illustrate that process-driven size-density relationships together with systematic initial size variation can result in different measured spectra (**Fig. 4**). For each case, **Figure 4** shows the age and size distribution of quartz and zircon grains from two source regions (column I). The two sources are combined, and then filtered according to a size-density relationship corresponding to a set of depositional conditions (column II). 100 zircon grains and 100 quartz grains are selected from each pool according to the probability of deposition determined by the depositional filter. This selection is repeated 10,000 times, and the median and 95% confidence interval of all results are determined (column III). Across all runs, the proportion of quartz and zircon grains deposited that come from each source region are shown in pie charts within column III.

Base Case

Results from the base case provide a point of comparison for other cases because all parameters, except for the age of detrital zircon grains, are consistent between the two sources. The measured age spectra for all size-density relationships accurately record the 1:1 sediment input for both quartz and zircon grains with no effect from transport process.

Case 1

Case 1 is identical to the base case except that Source 2 zircons are smaller than Source 1 grains. The resulting "deposits" show a range of spectra with shifting Source 1 and Source 2 inputs based on grain size. The "grain shielding" deposit shows an average of 85% Source 2 input, whereas the "equal sizes" case shows nearly 100% Source 1 input, with <0.1% Source 2 input. Deposits formed from the settling of grains through air and water both show a majority of Source 1 (larger) grains, but with differences in the proportion of the sources. The case shown for settling through air has 6% Source 2 grains on average and the case shown for settling through water has 35% Source 2 grains on average. Across all transport processes, quartz grains in the deposit are split evenly between the source regions.

Case 2

Case 2 explores process-dependent grain size shifts at smaller quartz and zircon grain sizes than Case 1. Deposits show a range of spectra with variable contributions from Source 1 and Source 2. At one extreme, the "grain shielding" case contains a slight majority of Source 2 grains. The other three transport cases show the opposite trend, with more Source 1 grains than Source 2 grains. Both the air and water settling cases contain a majority of Source 1 grains, but fewer Source 1 grains than the "equal size" case, which contains more than 80% Source 1 grains.

Rainstorm sample characterization

Geochronology

Age spectra from combined new and previously published (Schoenborn et al., 2012; Muhlbauer et al., 2017) zircon ages, as well as grain size measurements, are shown in **figures 5 and 6**. Four primary subpopulations (~1.0-1.2 Ga; ~1.3-1.5 Ga; ~1.6-1.9 Ga; and >2.0 Ga) are present. These subpopulations are interpreted to have their origin in the Grenville orogen (~1.0-1.2 Ga); the midcontinent (~1.3-1.5 Ga); the Yavapai-Mazatzal or Central Plains regions (~1.6-1.9); and older cratonic sources (>2.0 Ga) (Dickinson and Gehrels, 2009). The relative contribution of Grenville-aged material waxes and wanes through the section. This peak is absent or minimal in the Lower Johnnie, Rainstorm crystal fans, and upper Stirling Quartzite. It is particularly pronounced in the Wood Canyon Formation, as others note (Stewart et al., 2001; Muhlbauer et al., 2017).

Zircon size characterization

We document that Grenville-aged grains are, on average, larger than their Paleoproterozoic counterparts (**Fig. 6**). Zircon grains from the sub-Rainstorm sandstone and Rainstorm carbonate are distinctly finer than other samples. To assess if the detrital zircon population is susceptible to size-age fractionation by hydraulic effects, we split all measured detrital zircons into four size groups based on the length of their major axis (silt, very fine sand, fine sand, and medium sand, (Malusà et al., 2013; Malusà and Garzanti, 2019). The empirical cumulative distribution functions of these four size groups are shown in **Figure 7**. We assessed the null hypothesis that these size groups were drawn from the same age distribution using the Kolmogorov-Smirnov method (**Table 4).** Our data do not reject the null hypothesis for two pairs of grain size groups: first, silt and very fine sand, and second, fine sand and medium sand. Our data support the alternative hypothesis that both the silt and very fine sand groups have a different age distribution when each is compared to the fine sand and medium sand groups.

Crystal fan detritus characterization

The densities of the crystal fan detrital light and heavy fractions are shown in **Table 2**, as well as the relative proportions that fall into the light and heavy fractions are shown in **Table 2**. The Rainstorm crystal fan detritus is extremely unusual: the majority of the sediment, by both volume and mass, was separated into the heavy fraction during heavy liquids separation using methyl-iodide. A more typical split between the heavy and light fractions of a sedimentary sandstone would be on the order of 1% or less.

The density of the light fraction (ρ = 2.62 g/cm^3) is similar to that of quartz (ρ = 2.65 g/cm^3) and feldspar minerals (ρ = 2.55 to 2.78 g/cm^3). The density of the heavy fraction (ρ = 3.19 g/cm^3) is slightly less than that of methylene iodide (ρ = 3.32 g/cm^3), the heavy liquid used to separate the detrital minerals. It is possible that the methylene iodide, which had been previously used and recycled in an active mineral separation lab, was incompletely reclaimed following mixing with ethanol, and so the heavy liquid used in this separation was less dense than reported by the manufacturer. It is also possible that grain-grain interactions during settling of this unusual sediment enriched in heavy minerals resulted in sediment clumping or dragging, with some light grains sinking to the bottom, or that some air remained in the pore spaces of sediment during displacement with water, leading to a too-low density measurement.

Grain size data for both the heavy and light crystal fan detrital fractions are shown in **Table 2** and in **Figure 8**. The heavy fraction D_{50} grain size (43.1 μm) is much finer than the light fraction D_{50} grain size (64.9 μm). The predicted heavy grain size, based on the four size-density relationships used in **Figure 4** (equal-sized heavy mineral grains, "grain shielded" small heavy mineral grains, water settling, and air settling) and the measured density of the heavy fraction, is shown in **Table 3** along with the difference between these calculated grain sizes and the measured grain size. The heavy fraction D_{50} grain size is finer than predicted by all size-density relationships predicted here, but is closest to the "grain shielding" case using the size-density relationship quantified in Garzanti et al. (2008) from measurement of a modern aeolian sand.

Modeling size-provenance relationships in the Ediacaran-Terreneuvian Death Valley succession

Modeled results shown in **Figure 9** show the outcome of size-dependent selection of grain sizes drawn from this succession. As the grain size of the modeled deposit increases, the relative size and contribution of Grenville-aged grains to the resulting spectra also do. At a depositional grain size range of 69 ± 16 μm, between 2.4% and 20.3% (95% confidence interval) of the total spectra came from Grenville-aged (between 1 and 1.2 Ga) sources. 5.4% of the total crystal fan spectra comes from Grenville-aged sources, falling within this confidence interval. At a depositional grain size range of 154 ± 50 μm, between 19.7% and 55.3% (95% confidence interval) of the total spectra came from Grenville-aged (between 1 and 1.2 Ga) sources. 72.4% of the Wood Canyon Formation sample comes from Grenville-aged sources, well outside the 95% confidence interval identified here.

DISCUSSION

Process in an idealized sedimentary system

Results from our model of source mixing and transport-dependent grain size sorting and deposition highlight that transport process may generate offsets between the detrital zircon and bulk sediment histories in a sample. Such decoupling has been observed between quartz and zircon in an ancient basin (Augustsson et al., 2019). This new model provides a framework for exploring the causes and consequences of such decoupling.

Base case

In this case, with grain size held equal between the two sources, the resulting detrital zircon spectra match the quartz sources well. They are a faithful and quantitative record of sediment source regardless of transport process on average, although randomness within individual spectra can still lead to discrepancies between the true and the measured provenance record. Some of the parameters held constant in this simulation—including consistent zircon fertility and constant grain size between source regions—may often not be equal between source regions in natural settings.

Case 1

In this case, an initial difference in the average detrital zircon size of two populations resulted in a wide range of resultant age spectra. The resulting spectra cover a range of possibilities, from mostly Source 2 to all Source 1, depending on the transport process, and therefore the size-density relationship of the deposit. The ratios of source areas based on zircons do not always quantitatively capture the bulk sediment record.

Case 2

As in Case 1, an initial difference between detrital zircon populations results in a range of spectra due to size-sorting by transport process. The spectra range from mostly Source 1 grains to mostly Source 2 grains. The ratios of source areas based on zircons do not always quantitatively capture the bulk sediment record.

Because of the grain size-dependency of the size-density relationship, changes in grain size due to transport process are smaller at these smaller sediment sizes. One consequence of this is that even very small differences between detrital zircon population sizes can affect the outcome of the spectra, if the grain sizes are very close to the depositional sizes for zircon. The other consequence is that if grains are far outside the depositional window (for example, in this case a zircon source with an average size much larger than the 30-40 micron grains that are deposited), they will not be represented in the deposit.

Process in provenance records

These results demonstrate that transport process can impart a signature to the detrital zircon record of sediment if there are systematic differences in grain size between zircon populations. The properties of the transport medium, as well as grain-grain and grain-bed interactions, play a role in defining the size-density relationship of mineral grains in a deposit.

Each case explores how transport process could impart different signatures relative to the same bulk quartz grain size. Size-density relationships are unlikely to remain constant through a succession. For example, strata may oscillate between a size-density relationship controlled primarily by settling to a size-density relationship affected by selective entrainment, as observed by Steidtmann and Haywood (1982). Grain size also varies within a stratigraphic succession. In natural sediments, both bulk sediment size and size-density relationships change through a succession, mixing and matching different size-density relationships across grain sizes. In the context of this simple model, this might be analogized by moving from the Case 1 "grain shielding" spectra measured in a sandstone deposited from traction to a Case 2 "settling through water" siltstone layer. The synthetic spectra in these two cases differ in the relative contribution of zircons from different source areas but are identical in bulk sediment provenance. The complexity of real spectra will be greater than the simple examples shown here, as they typically contain more than two sources, and the zircon grain size distributions of real zircons are likely more complex than the generalized normal distributions used here.

Analysis of modern rivers suggests that the presence of a population, rather than the size of that population, is more significant in the interpretation of detrital zircon spectra (Link et al., 2005). Our study supports this conclusion, suggesting that differences in grain size may affect the size of a population without necessarily requiring a change in provenance. However, we also note that under some conditions, detrital zircons from a particular source may not be deposited in a unit at all, depending on size characteristics.

The Ediacaran-Terreneuvian succession of Death Valley

Detrital zircon size

Analysis of our dataset show that it is susceptible to hydrodynamic sorting (**Figure 7, Table 4**). Across all grains considered here, Grenville-aged grains are the largest on average (median long axis size of 160 μm). Other detrital zircon grains are somewhat smaller (median long axis size of 122 μm for grains between 1.2 and 1.5 Ga and 112.7 μm for grains between 1.5 and 1.9 Ga) and the oldest grains (older than 1.9 Ga) have the smallest median long axis size within the dataset (103.2 μm) (**Figure 6**). There is substantial overlap in sizes between these age ranges. Large and small zircons occur within each age bin, and the age of an individual grain cannot be derived from its size alone. However, an overall trend of average grain size decreasing with grain age is clear. A similar trend is noted within other datasets collected on other continents (Lawrence et al., 2011; Yang et al., 2012).

One hypothesis consistent with these data is that older zircon grains are subject to more sedimentary cycles, and erosion and abrasion results in a smaller average size. Another hypothesis is that there is been time-bound variation in the sizes to which zircons grow through Earth history. This suggestion is consistent with the observation that Zr concentrations have increased in Earth's continental igneous rocks through time and that overall zircon abundance has increased over the last 4 Ga (Keller et al., 2017). If zircon size is linked to Zr concentration and abundance, which seems probable based on observations of the high-Zr Grenville-aged granites that also produce abundant, large zircons (Moecher and Samson, 2006; Liu et al., 2017; Samson et al., 2018), then secular variation in average igneous zircon size could result. This systematic variation could then impact the detrital zircon record. Limited available grain size data for detrital and igneous zircon grains across Earth history makes further assessment of this hypothesis challenging.

Grenville sources

Figure 6 shows that Grenville-aged grains are large relative to other detrital zircon populations. This result is consistent with reports that Grenville zircons are large (Moecher and Samson, 2006) and with observations that both Grenville rocks in particular, and igneous rocks connected to the assembly of Rodinia in general, are Zr-rich (Liu et al., 2017; Samson et al., 2018). One impact of this is that as simulated spectra are generated for coarser and coarser samples, the relative contribution or peak associated with Grenville-aged sources increases **(Figure 9).** To some degree, changing grain size, rather than any change in sediment provenance, may be responsible for changing the contribution of Grenville-aged zircons between samples. This is perhaps best illustrated by the relatively fine-grained Rainstorm samples, which have minor Grenville-aged peaks and are the finest samples studied. Although the lack of a prominent Grenville-aged peak in these samples may truly reflect a lack of Grenville-aged sources, our analysis shows that this is a non-unique explanation. **Figure 9** demonstrates that synthetic spectra randomly chosen from the suite of zircons analyzed through the succession with a similar depositional grain size will also have minor to absent Grenville-aged peaks. These results are consistent with the Nd isotope analyses done by Schoenborn et al. (2012) which suggests a Yavapai-Matzatzal source for the Rainstorm Member. As in that study, these data cannot definitively rule out a cryptic Grenville source (Schoenborn et al., 2012); a Grenville source may not be represented in the detrital zircon record because of sediment sorting. The minor Grenville-aged peaks in both samples above and below this unit, combined with the potential for a "missing" Grenville peak in the Rainstorm crystal fans controlled by grain size, suggest that Grenville sources could have been minor but persistent through the interval.

The prominent Grenville-aged peak in the Wood Canyon Formation noted by Stewart et al. (2001) was the special focus of Muhbauer et al. (2017), which found no evidence for grain size sorting exerting a strong control on the presence of the Grenville-aged peak. We note that the Wood Canyon Formation zircons are the coarsest population examined in this study. As seen in **Figure 9**, synthetic spectra with a coarser grain size will develop more prominent Grenville-aged peaks. However, none of these synthetic spectra—even the coarsest, which takes the mean and standard deviation of its depositional size from the Wood Canyon Formation sample—reaches the same magnitude Grenville-aged peak. This suggests that, although grain size may indeed contribute to the substantial Grenville-aged peak seen in the Wood Canyon Formation, grain size alone does not account for it. In another example, grain size alone is also unlikely to account for the minimal or absent Grenville-aged peak seen in the upper Stirling Quartzite or lowermost Johnnie Formation; synthetic spectra coarser than 100 μm have clear Grenville-aged peaks **(Figure 9).** These data support the conclusion that shifts in the sandstones may represent genuine shifts in provenance (Schoenborn et al., 2012; Muhlbauer et al., 2017), though we note that fine-grained samples from these units are not included in this study. It is possible that size influence would be apparent in a finer-grained sample suite from these units.

These results support the case that change in detrital zircon spectra cannot be *prima facie* understood as evidence for changes in provenance (Lawrence et al., 2011; Ibañez-Mejia et al., 2018). In some cases, gaps or peaks in detrital zircon age spectra may be understood as either a change in provenance or a shift in grain size or a shift in sedimentary processes. Considering both age and grain size together can either highlight the non-unique interpretations of a detrital record or bolster the case for true changes in provenance.

Process and provenance in Rainstorm Member crystal fans

Previous studies have investigated the effect of size sorting on detrital zircon spectra in both modern and ancient examples (Hietpas et al., 2011b; Lawrence et al., 2011; Slama and Kosler, 2012; Augustsson et al., 2017; Muhlbauer et al., 2017; Ibañez-Mejia et al., 2018; Malkowski et al., 2019; Leary et al., 2020). This study integrates detrital zircon data through a succession in both fine and coarse-grained material. As described above, we find evidence that grain size can exert control on the detrital zircon spectra in our dataset, in particular for the size of the Grenville-aged peak in fine-grained samples. We also characterize how the grain size of detrital zircons within a sediment can depend—both in an absolute sense, and relative to the average bulk sediment grain size—on the transport processes involved. Changes in transport process, and the type of grain-grain or grain-bed interactions, can yield changes in the detrital zircon grain size within a sample by affecting the size-density distribution of the sediment. Here, we investigate the size-density distribution of detrital sediment within the Rainstorm crystal fans to further elucidate environmental conditions during their deposition.

Rainstorm Member zircons and sediments are, on average, finer than other units within this succession—consistent with Rainstorm Member deposition during an interval of maximum flooding (Summa, 1993; Bergmann et al., 2011, 2013). Examining the measured grain size offsets between the heavy and light detrital fractions of Rainstorm crystal strata is puzzling (Table 3). The heavy fraction is finer than the fine fraction, as expected—but it is much finer than would be predicted for either settling in air or in water. It is also much finer than would be predicted by the grain size-density relationship quantified by Garzanti et al. (2009) from observation of aeolian dunes, showing that selective entrainment in the Rainstorm yielded a different size-density relationship with a larger size change at lower densities. Entrainment equivalence between mineral grains has been expressed as a function of grain size, mineral and fluid density, shape, stacking pattern, and bed roughness (Komar, 2007) although the relationship remains largely empirically untested. The subaqueous depositional setting of the Rainstorm Member, and resulting greater density contrast between heavy and light minerals compared to subaerial settings, seems to have played a role in defining a more extreme size-density relationship compared to the modern aeolian dunes studied by Garzanti et al. (2008).

Sedimentary structures within the Rainstorm Member can provide information about flow regime and bed roughness during its deposition. The Rainstorm Member contains special hummocky cross-stratification and amalgamated scours interpreted as evidence for intermittent, high-energy storm events, as well as abundant storm-generated edgewise conglomerates (Summa, 1993; Pruss et al., 2008; Bergmann et al., 2013). Both discontinuous laminae within scours and intraclast beds form from periodic erosion, reworking, and deposition of sediment. This suggests that extensive reworking of sediment occurred episodically within the Rainstorm Member. The formation of heavy mineral-rich placer sands within the swash zone of beaches during storm events has been documented in modern settings (Woolsey et al., 1975; Komar and Wang, 1984)

The centimeter-scale crystal fans growing up from the sediment-water interface within the Rainstorm Member could act as baffles for sediment, increasing bed roughness and shielding fine grains from entrainment. Crystal fans are often found with mineral grains in inter-blade fill (note gray, heavy mineral-rich zones in interstitial spaces of crystal fan in **Figure 3**) (Summa, 1993; Pruss et al., 2008; Bergmann et al., 2013). Entrainment and settling of sediment as it passes over a rough bed leads to the formation of heavy mineral-enriched deposits in the interstices of gravel beds in some modern placers (Slingerland and Smith, 1986; Day and Fletcher, 1991); possibly the interstices of crystal fans protruding from the sediment-water interface could play a similar role. The importance of the crystal fans as sedimentary baffles in forming this heavy-mineral enriched deposit could be assessed by evaluating the heavy mineral enrichment, if any, in Rainstorm sandstones. Because the crystal fans often nucleate on and grow from the heavy mineral-rich deposits—thus postdating them—they may play a secondary role in its formation, if they play a role at all.

Rapid cementation of detrital mineral grains in a carbonate-precipitating environment could enhance selective entrainment by cementing grains in place. This early cementation would impact smaller grains, regardless of their density, to a greater degree than larger grains. Carbonate cementation of siliciclastic deposits is ubiquitous through the Rainstorm Member (Summa, 1993). In a study of amalgamated scours within the Rainstorm Member, Summa (1993) suggested that a high degree of sediment cohesion, potentially generated by carbonate cementation, was required to allow the high-angle scour walls, indicating that cementation occurred rapidly following deposition.

Thus, selective entrainment due to flow characteristics and bed roughness, and potentially enhanced by rapid carbonate cementation, is consistent with the observed size-density relationship in Rainstorm crystal fan detritus. The observed enrichment in heavy minerals seen in these deposits is also consistent with winnowing of sediment and removal of low-density grains by selective entrainment. Further supporting the role of selective entrainment is the provenance data from the unit, which is typical for the succession—demonstrated by both Nd (Schoenborn et al., 2012) and detrital zircon data to be consistent with expectations for a Laurentian passive margin, and wholly consistent with provenance throughout the succession. The unusual character of the siliciclastic material contained in these strata does not appear to be the result of an unusual sediment source, but of a set of transport processes operating on a siliciclastic deposit to yield an unusual deposit. Winnowing and selective entrainment, combined with low sediment supply, are consistent with other work on the origin of these deposits (Bergmann et al., 2013). In the Rainstorm crystal fan strata, grain shielding effects led to the deposition of an especially fine-grained set of detrital zircon grains. These grain-size effects may have contributed to the minimal Grenville-aged peak seen in these units.

Previous work suggested an aeolian source for the heavy mineral-rich silt-sized detritus within Rainstorm Member crystal fans because of the grain size, grain mineralogy and depositional style (Bergmann et al., 2013). The observed size-density relationships in these minerals do not conform with predictions for grains settling through air (**Table 3**) (Bagheri and Bonadonna, 2016; Raffaele et al., 2020). However, sedimentological evidence indicates extensive, storm-influenced reworking of Rainstorm sediment (Summa, 1993; Pruss et al., 2008; Bergmann et al., 2013). Because the size-density relationships of sediments reflect their most recent environment (Hand, 1967), any initial air-settling size-density relationship could be overprinted following deposition and reworking in a submarine environment. The winnowing of light minerals by wind from beach dunes is implicated in the formation of some modern beach placer deposits (Woolsey et al., 1975) and may have influenced the Rainstorm Member. The lack of a size-density relationship consistent with settling through air neither rules out nor requires an aeolian influence on siliciclastic detritus the Rainstorm Member.

The Rainstorm Member and the Shuram excursion

One of the motivations for study of the Rainstorm Member is understanding the sedimentological and environmental context of strata that record Earth's most negative carbon isotope excursion. This study has investigated the Rainstorm Member's provenance using detrital zircon and quantified the size-density relationship of siliciclastic detritus within carbonate crystal fan-bearing units. Our data suggest that the provenance of the Rainstorm Member, despite the unusual, heavy mineral-enriched deposits found within, are entirely consistent with provenance throughout the succession. This indicates that the formation of these deposits was the result of sediment transport processes occurring alongside deposition, rather than erosion of a distinct source not represented elsewhere in the succession. Sedimentological evidence for frequent and energetic storm activity indicates that sediment reworking was ongoing through deposition of the unit (Summa, 1993; Pruss et al., 2008). Climate can also influence the composition of clastic deposits (Johnsson, 1993). Available data suggest that the Johnnie Formation did not undergo cold-weather weathering and that it represents moderate to intense weathering of granitoid sources (Schoenborn and Fedo, 2011). Weathering products and elemental compositions were not measured as part of this study.

To date, no comparable heavy mineral suite has been reported in other Shuram excursion-bearing strata. In the course of this study, a sample of carbonate-cemented siltstone from the Shuram Formation of Oman was disaggregated through dissolution of the carbonate matrix and separated using heavy liquids (**Data Repository**). The Shuram Formation siltstone shares some characteristics with Rainstorm Member detritus: a coarse silt grain size, carbonate cement, abundant mica, and ample sedimentological evidence for storm action (McCarron, 1999; Le Guerroué et al., 2006b, 2006a; Grotzinger et al., 2011; Bergmann, 2013). In both Oman (McCarron, 1999; Le Guerroué et al., 2006b, 2006a; Bergmann, 2013) and Death Valley (Corsetti and Kaufman, 2003; Corsetti et al., 2004; Kaufman et al., 2007; Pruss et al., 2008; Bergmann, 2013), the carbonate strata recording the Shuram excursion include oolite and edgewise conglomerate interbedded with purple or red siltstone. Despite these similarities, the Shuram Formation siltstone was not enriched in heavy minerals. Only about a dozen grains were found in the heavy fraction following separation by heavy liquids and no size-density relationship was measured.

This difference between the Shuram Formation and the Rainstorm Member could be explained, in part, by differences in sediment delivery between the two locations. Limited sediment supply is linked to the formation of heavy mineral-enriched deposits in the Rainstorm Member (Bergmann et al., 2013). The Rainstorm Member is 50-100 meters thick (Stewart, 1970; Summa, 1993; Bergmann et al., 2013); the strata in Oman that contain the Shuram excursion (Shuram and Buah formations) are 500-600 meters thick in outcrop (McCarron, 1999). Assuming a synchronous excursion in Oman and Death Valley, this implies depositional rates in Oman were more than an order of magnitude greater, and that sediment supply was higher and potentially incompatible with formation of heavy mineral-enriched deposits by winnowing and selective entrainment in a sediment-starved setting. These observations of finer grain sizes, decreased sediment supply, and extensive sediment reworking and winnowing are consistent with interpretations of Rainstorm Member deposition during an interval of maximum flooding (Summa, 1993; Bergmann et al., 2011, 2013). Other similarities between the Rainstorm Member and other Shuram excursion-bearing successions, including the abundance of siltstone (often carbonate-cemented) and evidence for storm activity (McCarron, 1999; Le Guerroué et al., 2006a, 2006b; Grotzinger et al., 2011; Bergmann, 2013; Husson et al., 2015), remain intriguing.

CONCLUSION

Drawing on insights from draws on insights from process sedimentology, we demonstrate that sediment transport processes, from simple settling through fluid to selective entrainment, may lead to differential biases in detrital zircon records. Recognition that detrital zircon grains are not perfect records of provenance, but transported grains subject to sedimentary processes, encourages greater complexity and care in interpretations of provenance from these records. In the specific case study explored here, we find evidence that detrital zircon grains from the Ediacaran-Terrenuevian succession of Death Valley are susceptible to hydrodynamic fractionation. The effects of hydrodynamic fractionation are especially relevant for the relative contribution of Grenville-aged (1.0-1.2 Ga) zircon grains which are, on average, larger than older grains. The Rainstorm Member, which is geochemically, sedimentologically, and mineralogically unusual, nevertheless has a typical sediment provenance compared to other units in the succession, with substantial input from Yavapai-Mazatzal sources and a potentially cryptic Grenville source due to its fine grain size. The size-density relationship of detrital minerals and heavy mineral enrichment within carbonate strata of the Rainstorm Member are consistent with selective entrainment and winnowing of sediment during storms and low sediment supply during deposition.

ACKNOWLEDGMENTS

We thank S. Maclennan, S. Pruss, B. Schoene, M. Chia and D. Jones for assistance in the field and/or lab, and C. Keinitz for lodging. Thank you to J.G. Muhlbauer, who generously clarified grain size-age relationships previously published in Muhlbauer et al. 2017. M.D.C. was funded by a National Defense Science and Engineering Graduate Fellowship. K.D.B. received support from the Packard Foundation. Thanks to Gerilyn Soreghan and Mehrdad Sardar Abadi at the University of Oklahoma for assistance running LPSA samples.

Data Availability

All data and code related to this project are available at https://github.com/mcantine/rainstorm-zircons.

References

Abolins, M., Oskin, R., Prave, T., Summa, C., and Corsetti, F., 2000, Neoproterozoic glacial record in the Death Valley region, California and Nevada: GSA Field Guides, v. 2, p. 319–336, doi:10.1130/0-8137-0002-7.319.

Ader, M., Macouin, M., Trindade, R.I.F., Hadrien, M.H., Yang, Z., Sun, Z., and Besse, J., 2009, A multilayered water column in the Ediacaran Yangtze platform? Insights from carbonate and organic matter paired $\delta 13C$: Earth and Planetary Science Letters, v. 288, p. 213–227, doi:10.1016/j.epsl.2009.09.024.

Allwood, A.C., Grotzinger, J.P., Knoll, A.H., Burch, I.W., Anderson, M.S., Coleman, M.L., and Kanik, I., 2009, Controls on development and diversity of Early Archean stromatolites.: Proceedings of the National Academy of Sciences, v. 106, p. 9548–55, doi:10.1073/pnas.0903323106.

Augustsson, C., Aehnelt, M., Voigt, T., Kunkel, C., Meyer, M., and Schellhorn, F., 2019, Quartz and zircon decoupling in sandstone: Petrography and quartz cathodoluminescence of the Early Triassic continental Buntsandstein Group in Germany: Sedimentology, v. 66, p. 2874–2893, doi:10.1111/sed.12620.

Augustsson, C., Voigt, T., Bernhart, K., Kreißler, M., Gaupp, R., Gärtner, A., Hofmann, M., and Linnemann, U., 2017, Zircon size-age sorting and source-area effect : The German Triassic Buntsandstein Group: Sedimentary Geology, doi:10.1016/j.sedgeo.2017.11.004.

Babinski, M., Vieira, L.C., and Trindade, R.I.F., 2007, Direct dating of the Sete Lagoas cap carbonate (Bambuí Group, Brazil) and implications for the Neoproterozoic glacial events: Terra Nova, v. 19, p. 401–406, doi:10.1111/j.1365-3121.2007.00764.x.

Bagheri, G., and Bonadonna, C., 2016, On the drag of freely falling non-spherical particles: Powder Technology, v. 301, p. 526–544, doi:10.1016/j.powtec.2016.06.015.

Bergmann, K.D., 2013, Constraints on the carbon cycle and climate during the early evolution of animals: California Institute of Technology.

Bergmann, K.D., Grotzinger, J.P., and Fischer, W.W., 2013, Biological Influences on Seafloor Carbonate Precipitation: Palaios, v. 28, p. 99–115, doi:10.2110/palo.2012.p12-088r.

Bergmann, K.D., Zentmyer, R.A., and Fischer, W.W., 2011, The stratigraphic expression of a large negative carbon isotope excursion from the Ediacaran Johnnie Formation, Death Valley: Precambrian Research, v. 188, p. 45–56, doi:10.1016/j.precamres.2011.03.014.

Bjerrum, C.J., and Canfield, D.E., 2011, Towards a quantitative understanding of the late Neoproterozoic carbon cycle: Proceedings of the National Academy of Sciences of the United States of America, v. 108, p. 5542–5547, doi:10.1073/pnas.1101755108.

Blum, M.D., Milliken, K.T., Pecha, M.A., Snedden, J.W., Frederick, B.C., and Galloway, W.E., 2017, Detrital-zircon records of Cenomanian, Paleocene, and Oligocene Gulf of Mexico drainage integration and sediment routing: Implications for scales of basin-floor fans: Geosphere, v. 13, p. 2169–2205, doi:10.1130/GES01410.1.

Bold, U., Smith, E.F., Rooney, A.D., Bowring, S.A., Buchwaldt, R., Dudás, F.O., Ramezani, J., Crowley, J.L., Schrag, D.P., and Macdonald, F.A., 2016, Neoproterozoic stratigraphy of the Zavkhan terrane of Mongolia: The backbone for Cryogenian and early Ediacaran chemostratigraphic records: American Journal of Science, v. 315, p. 1–63,

doi:10.2475/01.2016.01.
Bowring, S.A., Grotzinger, J.P., Condon, D.J., Ramezani, J., Newall, M.J., and Allen, P.A., 2007, Geochronologic constraints on the chronostratigraphic framework of the Neoproterozoic Huqf Supergroup, Sultanate of Oman: American Journal of Science, v. 307, p. 1097–1145, doi:10.2475/10.2007.01.
Brady, L.L., Jobson, H.E., and Mckelvey, V.E., 1973, An Experimental Study of Heavy-Mineral Segregation Under Alluvial-Flow Conditions:
Briggs, L.I., 1965, Heavy Mineral Correlations and Provenances: Journal of Sedimentary Petrology, v. 35, p. 939–955.
Bristow, T.F., and Kennedy, M.J., 2008, Carbon isotope excursions and the oxidant budget of the Ediacaran atmosphere and ocean: Geology, v. 36, p. 863–866, doi:10.1130/G24968A.1.
Burns, S.J., and Matter, A., 1993, Carbon isotopic record of the latest Proterozoic from Oman: Eclogae Geologicae Helvetiae, v. 86, p. 595–607.
C., M.A., Claoue-Long, J.C., and Berge, C., 1996, SHRIMP constraints on sediment provenance and transport history in the Mesozoic Statfjord Formation, North Sea: Journal of the Geological Society, v. 153, p. 915–929, doi:10.1144/gsjgs.153.6.0915.
Canfield, D.E., Knoll, A.H., Poulton, S.W., Narbonne, G.M., and Dunning, G.R., 2020, Carbon isotopes in clastic rocks and the Neoproterozoic carbon cycle: American Journal of Science, v. 320, p. 97–124, doi:10.2475/02.2020.01.
Cantine, M.D., Bergmann, K.D., and Knoll, A.H., 2020, Carbonates before skeletons: a database approach: Earth-Science Reviews,.
Carroll, D., 1953, Weatherability of Zircon: SEPM Journal of Sedimentary Research, v. Vol. 23, doi:10.1306/d4269562-2b26-11d7-8648000102c1865d.
Cawood, P.A., Hawkesworth, C.J., and Dhuime, B., 2012, Detrital zircon record and tectonic setting: Geology, v. 40, p. 875–878, doi:10.1130/G32945.1.
Cawood, P.A., Hawkesworth, C.J., and Dhuime, B., 2013, The continental record and the generation of continental crust: Bulletin of the Geological Society of America, v. 125, p. 14–32, doi:10.1130/B30722.1.
Cheng, N.-S., 1997, Simplified Settling Velocity Formula for Sediment Particle: Journal of Hydraulic Engineering, v. 123, p. 149–152.
Chew, D., O'Sullivan, G., Caracciolo, L., Mark, C., and Tyrrell, S., 2020, Sourcing the sand: Accessory mineral fertility, analytical and other biases in detrital U-Pb provenance analysis: Earth-Science Reviews, v. 202, p. 103093, doi:10.1016/j.earscirev.2020.103093.
Christie-Blick, N., and Levy, M., 1989, Concepts of Sequence Stratigraphy, with Examples from Strata of Late Proterozoic and Cambrian Age in the Western United States, *in* Late Proterozoic and Cambrian Tectonics, Sedimentation, and Record of Metazoan Radiation in the Western United States: Pocatello, Idaho, to Reno, Nevada 20–29 July, 1989,.
Clapham, M.E., and Corsetti, F.A., 2005, Deep valley incision in the terminal Neoproterozoic (Ediacaran) Johnnie Formation, eastern California, USA: Tectonically or glacially driven? Precambrian Research, v. 141, p. 154–164, doi:10.1016/j.precamres.2005.09.002.
Clift, R., and Gauvin, W.H., 1971, Motion of entrained particles in gas streams: The Canadian Journal of Chemical Engineering, v. 49, p. 439–448, doi:10.1002/cjce.5450490403.
Clifton, H.E., 1969, Beach lamination: Nature and origin: Marine Geology, v. 7, p. 553–559, doi:10.1016/0025-3227(69)90023-1.
Cloud, P.E., Wright, L.A., Williams, E.G., Diehl, P., and Walter, M.R., 1969, Giant stromatolites and associated vertical tubes from the upper Proterozoic Noonday Dolomite: Geological

Society of America Bulletin, v. 85, p. 1869–1882.

Corsetti, F.A., and Grotzinger, J.P., 2005, Origin and significance of tube structures in Neoproterozoic post-glacial cap carbonates: Example from Noonday Dolomite, Death Valley, United States: Palaios, v. 20, p. 348–362, doi:10.2110/palo.2003.p03-96.

Corsetti, F.A., and Hagadorn, J.W., 2000, Precambrian-Cambrian transition: Death Valley, United States: Geology, v. 28, p. 299–302, doi:10.1130/0091-7613(2000)028<0299:PCTDVU>2.3.CO;2.

Corsetti, F.A., and Kaufman, A.J., 2003, Stratigraphic investigations of carbon isotope anomalies and Neoproterozoic ice ages in Death Valley, California: Bulletin of the Geological Society of America, v. 115, p. 916–932, doi:10.1130/B25066.1.

Corsetti, F.A., Lorentz, N.J., and Pruss, S.B., 2004, Formerly-aragonite seafloor fans from Neoproterozoic strata, Death Valley and southeastern Idaho, United States: Implications for “cap carbonate” formation and Snowball Earth: Geophysical Monograph Series, v. 146, p. 33–44, doi:10.1029/146GM04.

Creveling, J.R., Bergmann, K.D., and Grotzinger, J.P., 2016, Cap carbonate platform facies model, Noonday Formation, SE California: Bulletin of the Geological Society of America, v. 128, p. 1249–1269, doi:10.1130/B31442.1.

Cui, H., Kaufman, A.J., Xiao, S., Zhou, C., and Liu, X.M., 2017, Was the Ediacaran Shuram Excursion a globally synchronized early diagenetic event? Insights from methane-derived authigenic carbonates in the uppermost Doushantuo Formation, South China: Chemical Geology, v. 450, p. 59–80, doi:10.1016/j.chemgeo.2016.12.010.

Darroch, S.A.F., Smith, E.F., La, M., and Erwin, D.H., 2018, Ediacaran Extinction and Cambrian Explosion: , p. 653–663, doi:10.1016/j.tree.2018.06.003.

Day, S.J., and Fletcher, W.K., 1991, Accumulation of High-density Minerals in Pavement Voids Formation of Gravel Pavement: Journal of Sedimentary Petrology, v. 61, p. 871–882.

Day, S.J., and Fletcher, W.K., 1989, Effects of valley and local channel morphology on the distribution of gold in stream sediments from Harris Creek, British Columbia, Canada: Journal of Geochemical Exploration, v. 32, p. 1–16, doi:10.1016/0375-6742(89)90040-X.

Derry, L.A., 2010, A burial diagenesis origin for the Ediacaran Shuram-Wonoka carbon isotope anomaly: Earth and Planetary Science Letters, v. 294, p. 152–162, doi:10.1016/j.epsl.2010.03.022.

Dickinson, W.R., 2008, Impact of differential zircon fertility of granitoid basement rocks in North America on age populations of detrital zircons and implications for granite petrogenesis: Earth and Planetary Science Letters, v. 275, p. 80–92, doi:10.1016/j.epsl.2008.08.003.

Dickinson, W.R., and Gehrels, G.E., 2009, U-Pb ages of detrital zircons in Jurassic eolian and associated sandstones of the Colorado plateau: Evidence for transcontinental dispersal and intraregional recycling of sediment: Bulletin of the Geological Society of America, v. 121, p. 408–433, doi:10.1130/B26406.1.

Diehl, P., 1979, The Stratigraphy, Depositional Environments, and Quantitative Petrography of the Precambrian-Cambrian Wood Canyon Formation, Death Valley: The Pennsylvania State University, 438 p.

Dietrich, W.E., 1982, Settling velocity of natural particles: Water Resources Research, v. 18, p. 1615–1626, doi:10.1029/WR018i006p01615.

Emery, K.O., and Stevenson, R.E., 1950, Laminated beach sand: Journal of Sedimentary Petrology, v. 20, p. 220–223.

Fedo, C.M., and Cooper, J.D., 1990, Braided fluvial to marine transition: the basal Lower Cambrian Wood Canyon Formation, southern Marble Mountains, Mojave Desert, California: Journal of Sedimentary Petrology, v. 60, p. 220–234.

Fedo, C.M., and Cooper, J.D., 2001, Sedimentology and sequence stratigraphy of Neoptoterozoic and Cambrian units across a craton-margin hinge zone, southeastern California, and implications for the early evolution of the Cordilleran margin: Sedimentary Geology, v. 141–142, p. 501–522, doi:10.1016/S0037-0738(01)00088-4.

Fedo, C.M., Sircombe, K.N., and Rainbird, R.H., 2003, Detrital zircon analysis of the sedimentary record: Reviews in Mineralogy and Geochemistry, v. 53, p. 277–303.

Ferguson, R.I., and Church, M., 2004, A simple universal equation for grain settling velocity: Journal of Sedimentary Research, v. 74, p. 933–937, doi:10.1306/051204740933.

Fike, D.A., Grotzinger, J.P., Pratt, L.M., and Summons, R.E., 2006, Oxidation of the Ediacaran ocean: Nature, v. 444, p. 744–747, doi:10.1038/nature05345.

Fisher, C.M., Vervoort, J.D., and Hanchar, J.M., 2014, Guidelines for reporting zircon Hf isotopic data by LA-MC-ICPMS and potential pitfalls in the interpretation of these data: Chemical Geology, v. 363, p. 125–133, doi:10.1016/j.chemgeo.2013.10.019.

Flowerdew, M.J., Fleming, E.J., Morton, A.C., Frei, D., Chew, D.M., and Daly, J.S., 2019, Assessing mineral fertility and bias in sedimentary provenance studies: examples from the Barents Shelf: Geological Society, London, Special Publications, p. SP484.11, doi:10.1144/sp484.11.

Friedman, G.M., 1961, Distinction between dune, beach, and river sands from their textural characteristics: Journal of Sedimentary Petrology, v. 31, p. 514–529.

Garzanti, E., Andò, S., and Vezzoli, G., 2009, Grain-size dependence of sediment composition and environmental bias in provenance studies: Earth and Planetary Science Letters, v. 277, p. 422–432, doi:10.1016/j.epsl.2008.11.007.

Garzanti, E., Andò, S., and Vezzoli, G., 2008, Settling equivalence of detrital minerals and grain-size dependence of sediment composition: v. 273, p. 138–151, doi:10.1016/j.epsl.2008.06.020.

Gehrels, G., 2014, Detrital Zircon U-Pb Geochronology Applied to Tectonics: Annual Review of Earth and Planetary Sciences, v. 42, p. 127–149, doi:10.1146/annurev-earth-050212-124012.

Gehrels, G.E., 2000, Introduction to detrital zircon studies of Paleozoic and Triassic strata in western Nevada and northern California: GSA Special Papers, v. 347.

Gibbs, R.J., Matthews, M.D., and Link, D.A., 1971, The relationship between sphere size and settling velocity: Journal of Sedimentary Petrology, v. 41, p. 7–18, doi:10.1017/CBO9781107415324.004.

Grigg, N.S., and Rathbun, R.E., 1965, Hydraulic equivalence of minerals with a consideration of the reentrainment process.: US Geological Survey Professional Paper, 650, p. B77–B80.

Grotzinger, J.P., Fike, D.A., and Fischer, W.W., 2011, Enigmatic origin of the largest-known carbon isotope excursion in Earth's history: Nature Geoscience, v. 4, p. 285–292, doi:10.1038/ngeo1138.

Grotzinger, J.P., and James, N.P., 2000, Precambrian Carbonates: Evolution of Understanding: Carbonate Sedimentation and Diagenesis in the Evolving Precambrian World, p. 3–20, doi:10.2110/pec.00.67.

Grotzinger, J.P., and Read, J.F., 1983, Evidence for primary aragonite precipitation, lower Proterozoic (1.9 Ga) Rocknest dolomite, Wopmay orogen, northwest Canada.: Geology, v.

11, p. 710–713, doi:10.1130/0091-7613(1983)11<710:EFPAPL>2.0.CO;2.

Le Guerroué, E., 2010, Duration and synchroneity of the largest negative carbon isotope excursion on Earth: The Shuram/Wonoka anomaly: Comptes Rendus - Geoscience, v. 342, p. 204–214, doi:10.1016/j.crte.2009.12.008.

Le Guerroué, E., Allen, P.A., and Cozzi, A., 2006a, Chemostratigraphic and sedimentological framework of the largest negative carbon isotopic excursion in earth history: The Neoproterozoic Shuram formation (Nafun Group, Oman): Precambrian Research, v. 146, p. 68–92, doi:10.1016/j.precamres.2006.01.007.

Le Guerroué, E., Allen, P.A., and Cozzi, A., 2006b, Parasequence development in the Ediacaran Shuram Formation (Nafun Group, Oman): High-resolution stratigraphic test for primary origin of negative carbon isotopic ratios: Basin Research, v. 18, p. 205–219, doi:10.1111/j.1365-2117.2006.00292.x.

Le Guerroué, E., Allen, P.A., Cozzi, A., and Etienne, J.L., 2006c, 50 Myr recovery from the largest negative δ13C excursion in the Ediacaran ocean: Terra Nova, v. 18, p. 147–153.

Guo, R., Hu, X., Garzanti, E., Lai, W., Yan, B., and Mark, C., 2020, How faithfully do the geochronological and geochemical signatures of detrital zircon, titanite, rutile and monazite record magmatic and metamorphic events? A case study from the Himalaya and Tibet: Earth-Science Reviews, v. 201, p. 103082, doi:10.1016/j.earscirev.2020.103082.

Hagadorn, J.W., and Waggoner, B., 2000, Ediacaran fossils from the southwestern Great Basin, United States: Journal of Paleontology, v. 74, p. 349–359, doi:10.1017/S0022336000031553.

Halverson, G.P., Hoffman, P.F., Schrag, D.P., Maloof, A.C., and Rice, A.H.N., 2005, Toward a Neoproterozoic composite carbon isotope record: Bulletin of the Geological Society of America, v. 117, p. 1181–1207, doi:10.1130/B25630.1.

Hand, B.M., 1967, Differentiation of Beach and Dune Sands, Using Settling Velocities of Light and Heavy Minerals: Journal of Sedimentary Petrology, v. Vol. 37, p. 514–520, doi:10.1306/74D71703-2B21-11D7-8648000102C1865D.

Hawkesworth, C.J., Cawood, P.A., Kemp, T., Storey, C., and Dhuime, B., 2009, A matter of preservation: Science, v. 323.

Hegenberger, W., 1987, Gas Escape Structures in Precambrian Peritidal Carbonate Rocks: , p. 53–59.

Hietpas, J., Samson, S., and Moecher, D., 2011a, A direct comparison of the ages of detrital monazite versus detrital zircon in Appalachian foreland basin sandstones: Searching for the record of Phanerozoic orogenic events: Earth and Planetary Science Letters, v. 310, p. 488–497, doi:10.1016/j.epsl.2011.08.033.

Hietpas, J., Samson, S., Moecher, D., and Chakraborty, S., 2011b, Enhancing tectonic and provenance information from detrital zircon studies: assessing terrane-scale sampling and grain-scale characterization: Journal of the Geological Society, v. 168, p. 309–318, doi:10.1144/0016-76492009-163.

Higgins, J.A., Fischer, W.W., and Schrag, D.P., 2009, Oxygenation of the ocean and sediments: Consequences for the seafloor carbonate factory: Earth and Planetary Science Letters, v. 284, p. 25–33, doi:10.1016/j.epsl.2009.03.039.

Hoffman, P.F., Halverson, G.P., and Grotzinger, J.P., 2002, Are Proterozoic cap carbonates and isotopic excursions a record of gas hydrate destabilization following Earth's coldest intervals?: Comment and Reply: Geology, p. 443–446, doi:10.1130/0091-7613(2001)029<0443:APCCAI>2.0.CO;2.

Hoffman, P.F., and Schrag, D.P., 2002, The snowball Earth hypothesis: testing the limits of global change: Terra, v. 14, p. 129–155, doi:10.1080/713604466.

Hofmann, H.J., and Jackson, G.D., 1987, Proterozoic ministromatolites with radial-fibrous fabric: Sedimentology, v. 34, p. 963–971, doi:10.1111/j.1365-3091.1987.tb00586.x.

Hogan, E.G., Fedo, C.M., and Cooper, J.D., 2011, Reassessment of the basal Sauk supersequence boundary across the Laurentian craton-margin hinge zone, Southeastern California: Journal of Geology, v. 119, p. 661–685, doi:10.1086/661990.

Husson, J.M., Maloof, A.C., Schoene, B., Chen, C.Y., and Higgins, J.A., 2015, Stratigraphic expression of earth's deepest δ13C excursion in the Wonoka formation of South Australia: American Journal of Science, v. 315, p. 1–45, doi:10.2475/01.201501.

Ibañez-Mejia, M., Pullen, A., Pepper, M., Urbani, F., Ghoshal, G., and Ibañez-Mejia, J.C., 2018, Use and abuse of detrital zircon U-Pb geochronology-A case from the Río Orinoco delta, eastern Venezuela: Geology, v. 46, p. 1019–1022, doi:10.1130/G45596.1.

James, N.P., Narbonne, G.M., and Kyser, T.K., 2001, Late Neoproterozoic cap carbonates: Mackenzie Mountains, northwestern Canada: precipitation and global glacial meltdown: Canadian Journal of Earth Sciences, v. 38, p. 1229–1262, doi:10.1139/e01-046.

Jiang, G., Kaufman, A.J., Christie-Blick, N., Zhang, S., and Wu, H., 2007, Carbon isotope variability across the Ediacaran Yangtze platform in South China: Implications for a large surface-to-deep ocean ??13C gradient: Earth and Planetary Science Letters, v. 261, p. 303–320, doi:10.1016/j.epsl.2007.07.009.

Johnsson, M.J., 1993, The system controlling the composition of clastic sediments: Special Paper of the Geological Society of America, v. 284, p. 1–19, doi:10.1130/SPE284-p1.

Johnston, D.T., MacDonald, F.A., Gill, B.C., Hoffman, P.F., and Schrag, D.P., 2012, Uncovering the Neoproterozoic carbon cycle: Nature, v. 483, p. 320–323, doi:10.1038/nature10854.

Kah, L.C., and Grotzinger, J.P., 1992, Early Proterozoic (1.9 Ga) thrombolites of the Rocknest Fm, NW Territories, Canada: Palaios, v. 7, p. 305–315.

Kah, L.C., and Knoll, A.H., 1996, Microbenthic distribution of Proterozoic tidal flats: Environmental and taphonomic considerations: Geology, v. 24, p. 79–82, doi:10.1130/0091-7613(1996)024<0079:MDOPTF>2.3.CO;2.

Kaufman, A.J., Corsetti, F.A., and Varni, M.A., 2007, The effect of rising atmospheric oxygen on carbon and sulfur isotope anomalies in the Neoproterozoic Johnnie Formation, Death Valley, USA: Chemical Geology, v. 237, p. 65–81, doi:10.1016/j.chemgeo.2006.06.023.

Kaufman, A.J., Jiang, G., Christie-Blick, N., Banerjee, D.M., and Rai, V., 2006, Stable isotope record of the terminal Neoproterozoic Krol platform in the Lesser Himalayas of northern India: Precambrian Research, v. 147, p. 156–185, doi:10.1016/j.precamres.2006.02.007.

Keller, C.B., Boehnke, P., and Schoene, B., 2017, Temporal variation in relative zircon abundance throughout Earth history: Geochemical Perspectives Letters, v. 3, p. 179–189, doi:10.7185/geochemlet.1721.

Knauth, L.P., and Kennedy, M.J., 2009, The late Precambrian greening of the Earth: Nature, v. 460, p. 728–732, doi:10.1038/nature08213.

Komar, P.D., 2007, The Entrainment, Transport and Sorting of Heavy Minerals by Waves and Currents: Developments in Sedimentology, v. 58, p. 3–48, doi:10.1016/S0070-4571(07)58001-5.

Komar, P.D., Clemens, K.E., Li, Z., and Shih, S.M., 1989, The effects of selective sorting on factor analyses of heavy-mineral assemblages: Journal of Sedimentary Petrology, v. 59, p. 590–596, doi:10.1306/212f8ff8-2b24-11d7-8648000102c1865d.

Komar, P.D., and Li, Z., 1988, Applications of grain-pivoting and sliding analyses to selective entrapment of gravel and to flow-competence evaluations: Sedimentology, v. 35, p. 681–695, doi:10.1111/j.1365-3091.1988.tb01244.x.

Komar, P.D., and Wang, C., 1984, Processes of selective grain transport and the formation of placers on beaches.: Journal of Geology, v. 92, p. 637–655, doi:10.1086/628903.

Lawrence, R.L., Cox, R., Mapes, R.W., and Coleman, D.S., 2011, Hydrodynamic fractionation of zircon age populations: Bulletin of the Geological Society of America, v. 123, p. 295–305, doi:10.1130/B30151.1.

Leary, R.J., Smith, M.E., and Umhoefer, P., 2020, Grain-Size Control on Detrital Zircon Cycloprovenance in the Late Paleozoic Paradox and Eagle Basins, USA: Journal of Geophysical Research: Solid Earth, v. 125, p. 1–19, doi:10.1029/2019JB019226.

Lee, C., Love, G.D., Fischer, W.W., Grotzinger, J.P., and Halverson, G.P., 2015, Marine organic matter cycling during the Ediacaran Shuram excursion: Geology, v. 43, p. 1103–1106, doi:10.1130/G37236.1.

Li, Z., Cao, M., Loyd, S.J., Algeo, T.J., Zhao, H., Wang, X., Zhao, L., and Chen, Z.-Q., 2020, Transient and stepwise ocean oxygenation during the late Ediacaran Shuram Excursion: Insights from carbonate δ238U of northwestern Mexico: Precambrian Research, v. 344, p. 105741, doi:10.1016/j.precamres.2020.105741.

Link, P.K., Fanning, C.M., and Beranek, L.P., 2005, Reliability and longitudinal change of detrital-zircon age spectra in the Snake River system, Idaho and Wyoming: An example of reproducing the bumpy barcode: Sedimentary Geology, v. 182, p. 101–142, doi:10.1016/j.sedgeo.2005.07.012.

Liu, C., Knoll, A.H., and Hazen, R.M., 2017, Geochemical and mineralogical evidence that Rodinian assembly was unique: Nature Communications, v. 8, p. 1–7, doi:10.1038/s41467-017-02095-x.

Lowright, R., Williams, E.G., and Dachille, F., 1972, An Analysis of Factors Controlling Deviations in Hydraulic Equivalence in Some Modern Sands: SEPM Journal of Sedimentary Research, v. Vol. 42, doi:10.1306/74d725e5-2b21-11d7-8648000102c1865d.

Ludwig, K.R., 2003, User's Manual for Isoplot 3.00 - A Geochronological Toolkit for Microsoft Excel: Berkeley Geochronology Center Special Publication, p. 71.

MacDonald, F.A., McClelland, W.C., Schrag, D.P., and MacDonald, W.P., 2009, Neoproterozoic glaciation on a carbonate platform margin in Arctic Alaska and the origin of the North slope subterrane: Bulletin of the Geological Society of America, v. 121, p. 448–473, doi:10.1130/B26401.1.

Macdonald, F.A., Prave, A.R., Petterson, R., Smith, E.F., Pruss, S.B., Oates, K., Waechter, F., Trotzuk, D., and Fallick, A.E., 2013a, The Laurentian record of Neoproterozoic glaciation, tectonism, and eukaryotic evolution in Death Valley, California: Bulletin of the Geological Society of America, v. 125, p. 1203–1223, doi:10.1130/B30789.1.

Macdonald, F.A., Strauss, J. V., Sperling, E.A., Halverson, G.P., Narbonne, G.M., Johnston, D.T., Kunzmann, M., Schrag, D.P., and Higgins, J.A., 2013b, The stratigraphic relationship between the Shuram carbon isotope excursion, the oxygenation of Neoproterozoic oceans, and the first appearance of the Ediacara biota and bilaterian trace fossils in northwestern Canada: Chemical Geology, v. 362, p. 250–272, doi:10.1016/j.chemgeo.2013.05.032.

Mackey, G.N., Horton, B.K., and Milliken, K.L., 2012, Provenance of the Paleocene-Eocene Wilcox Group, western Gulf of Mexico basin: Evidence for integrated drainage of the southern Laramide Rocky Mountains and Cordilleran arc: Bulletin of the Geological

Society of America, v. 124, p. 1007–1024, doi:10.1130/B30458.1.

Malkowski, M.A., Sharman, G.R., Johnstone, S.A., Grove, M.J., Kimbrough, D.L., and Graham, S.A., 2019, Dilution and propagation of provenance trends in sand and mud: Geochemistry and detrital zircon geochronology of modern sediment from central California (U.S.A.): American Journal of Science, v. 319, p. 846–902, doi:10.2475/10.2019.02.

Malusà, M.G., Carter, A., Limoncelli, M., Villa, I.M., and Garzanti, E., 2013, Bias in detrital zircon geochronology and thermochronometry: Chemical Geology, v. 359, p. 90–107, doi:10.1016/j.chemgeo.2013.09.016.

Malusà, M.G., and Garzanti, E., 2019, The sedimentology of detrital thermochronology, *in* Malusà, M.G. and Fitzgerald, P.G. eds., Fission-Track Thermochronology and its Application to Geology, Springer.

Malusà, M.G., Resentini, A., and Garzanti, E., 2016, Hydraulic sorting and mineral fertility bias in detrital geochronology: Gondwana Research, v. 31, p. 1–19, doi:10.1016/j.gr.2015.09.002.

Matthews, J.J., Liu, A.G., Yang, C., McIlroy, D., Levell, B., and Condon, D.J., 2020, A Chronostratigraphic Framework for the Rise of the Ediacaran Macrobiota: New Constraints from Mistaken Point Ecological Reserve, Newfoundland: GSA Bulletin, p. 1–13, doi:10.1130/b35646.1.

McCarron, M.E.G., 1999, The sedimentology and chemostratigraphy of the Nafun Group, Huqf Supergroup, Oman: Oxford University, 302 p.

McFadden, K.A., Huang, J., Chu, X., Jiang, G., Kaufman, A.J., Zhou, C., Yuan, X., and Xiao, S., 2008, Pulsed oxidation and biological evolution in the Ediacaran Doushantuo Formation.: Proceedings of the National Academy of Sciences of the United States of America, v. 105, p. 3197–3202, doi:10.1073/pnas.0708336105.

McIntyre, D.D., 1959, The Hydraulic Equivalence and Size Distributions of Some Mineral Grains from a Beach: The Journal of Geology, v. 67, p. 278–301.

McQuivey, R.S., and Keefer, T.N., 1969, The relation of turbulence to the deposition of magnetite over ripples, *in* Geological Survey Professional Paper 650-D,.

Melezhik, V.A., Roberts, D., Fallick, A.E., and Gorokhov, I.M., 2008, The Shuram - Wonoka event recorded in a high-grade metamorphic terrane: Insight from the Scandinavian Caledonides: Geological Magazine, v. 145, p. 161–172, doi:10.1017/S0016756807004189.

Minguez, D., Kodama, K.P., and Hillhouse, J.W., 2015, Paleomagnetic and cyclostratigraphic constraints on the synchroneity and duration of the Shuram carbon isotope excursion, Johnnie Formation, Death Valley Region, CA: Precambrian Research, v. 266, p. 395–408, doi:10.1016/j.precamres.2015.05.033.

Miyazaki, Y., Planavsky, N.J., Bolton, E.W., and Reinhard, C.T., 2018, Making Sense of Massive Carbon Isotope Excursions With an Inverse Carbon Cycle Model: Journal of Geophysical Research: Biogeosciences, v. 123, p. 2485–2496, doi:10.1029/2018JG004416.

Moecher, D.P., Kelly, E.A., Hietpas, J., and Samson, S.D., 2019, Proof of recycling in clastic sedimentary systems from textural analysis and geochronology of detrital monazite: Implications for detrital mineral provenance analysis: Bulletin of the Geological Society of America, v. 131, p. 1115–1132, doi:10.1130/B31947.1.

Moecher, D.P., and Samson, S.D., 2006, Differential zircon fertility of source terranes and natural bias in the detrital zircon record: Implications for sedimentary provenance analysis: Earth and Planetary Science Letters, v. 247, p. 252–266, doi:10.1016/j.epsl.2006.04.035.

Morton, A.C., and Hallsworth, C., 1994, Identifying provenance-specific features of detrital heavy mineral assemblages in sandstones: Sedimentary Geology, v. 90, p. 241–256, doi:10.1016/0037-0738(94)90041-8.

Morton, A.C., and Hallsworth, C., 2007, Stability of detrital heavy minerals during burial diagenesis, *in* Heavy Minerals in Use, p. 215–245.

Muhlbauer, J.G., Fedo, C.M., and Farmer, G.L., 2017, Influence of textural parameters on detrital-zircon age spectra with application to provenance and paleogeography during the Ediacaran−Terreneuvian of southwestern Laurentia: Geological Society of America Bulletin, p. B31611.1, doi:10.1130/b31611.1.

Muhlbauer, J.G., Fedo, C.M., and Moersch, J.E., 2020, Architecture of a distal pre-vegetation braidplain: Cambrian middle member of the Wood Canyon Formation, southern Marble Mountains, California, USA: Sedimentology, v. 67, p. 1084–1113, doi:10.1111/sed.12677.

Muscente, A.D., Boag, T.H., Bykova, N., and Schiffbauer, J.D., 2018, Environmental disturbance, resource availability, and biologic turnover at the dawn of animal life: Earth-Science Reviews, v. 177, p. 248–264, doi:10.1016/j.earscirev.2017.11.019.

Oehlert, A.M., and Swart, P.K., 2014, Interpreting carbonate and organic carbon isotope covariance in the sedimentary record: Nature Communications, v. 5, p. 4672, doi:10.1038/ncomms5672.

Petterson, R., Prave, A.R., Wernicke, B.P., and Fallick, A., 2011, The Neoproterozoic Noonday Formation, Death Valley region, California: Bulletin of the Geological Society of America, v. 123, p. 1317–1336, doi:10.1130/B30281.1.

Prave, A.R., 1999, Two diamictites, two cap carbonates, two d13C excursions, two rifts: The Neoproterozoic Kingston Peak Formation, Death Valley, California: Geology, v. 27, p. 339–342.

Pruss, S.B., Corsetti, F.A., and Fischer, W.W., 2008, Seafloor-precipitated carbonate fans in the Neoproterozoic Rainstorm Member, Johnnie Formation, Death Valley Region, USA: Sedimentary Geology, v. 207, p. 34–40, doi:10.1016/j.sedgeo.2008.03.005.

Pu, J.P., Bowring, S.A., Ramezani, J., Myrow, P., Raub, T.D., Landing, E., Mills, A., Hodgin, E., and Macdonald, F.A., 2016, Dodging snowballs: Geochronology of the Gaskiers glaciation and the first appearance of the Ediacaran biota: Geology, v. 44, p. 955–958, doi:10.1130/G38284.1.

Raffaele, L., Bruno, L., and Sherman, D.J., 2020, Statistical characterization of sedimentation velocity of natural particles: Aeolian Research, v. 44, p. 100593, doi:10.1016/j.aeolia.2020.100593.

Rittenhouse, G., 1943, Transportation and deposition of heavy minerals: Bulletin of the Geological Society of America, v. 54, p. 1725–1780.

Rodrigues Nogueira, A.C., Riccomini, C., Nóbrega Sial, A., Veloso Moura, C.A., and Fairchild, T.R., 2003, Soft-sediment deformation at the base of the Neoproterozoic Puga cap carbonate (southwestern Amazon craton, Brazil): Confirmation of rapid icehouse to greenhouse transition in snowball Earth: Geology, v. 31, p. 613–616, doi:10.1130/0091-7613(2003)031<0613:SDATBO>2.0.CO;2.

Rooney, A.D., Cantine, M.D., Bergmann, K.D., Gómez-Pérez, I., Al Baloushi, B., Boag, T.H., Busch, J.F., Sperling, E.A., and Strauss, J. V., 2020, Calibrating the coevolution of Ediacaran life and environment: Proceedings of the National Academy of Sciences of the United States of America, v. 117, p. 16824–16830, doi:10.1073/pnas.2002918117.

Rothman, D.H., Hayes, J.M., and Summons, R.E., 2003, Dynamics of the Neoproterozoic carbon cycle: Proceedings of the National Academy of Sciences, v. 100, p. 8124–8129, doi:10.1073/pnas.0832439100.

Rubey, W.W., 1933, Settling velocity of gravel, sand, and silt particles: American Journal of Science, v. s5-25, p. 325–338, doi:10.2475/ajs.s5-25.148.325.

Sallenger, A.H., 1979, Inverse grading and hydraulic equivalence in grain flow deposits.: Journal of Sedimentary Petrology, v. 49, p. 553–562, doi:10.1306/212F7789-2B24-11D7-8648000102C1865D.

Samson, S.D., Moecher, D.P., and Satkoski, A.M., 2018, Inherited, enriched, heated, or recycled? Examining potential causes of Earth's most zircon fertile magmatic episode: Lithos, v. 314–315, p. 350–359, doi:10.1016/j.lithos.2018.06.015.

Schoenborn, W.A., 2010, Geochemistry of the Neoproterozoic Johnnie Formation and Stirling Quartzite, southern Nopah Range, California: Deciphering the Roles of Climate, Tectonics, and Sedimentary Process in Reconstructing the Early Evolution of a Rifted Continental Margin: 322 p.

Schoenborn, W.A., and Fedo, C.M., 2011, Provenance and paleoweathering reconstruction of the Neoproterozoic Johnnie Formation, southeastern California: Chemical Geology, v. 285, p. 231–255, doi:10.1016/j.chemgeo.2011.04.014.

Schoenborn, W.A., Fedo, C.M., and Farmer, G.L., 2012, Provenance of the Neoproterozoic Johnnie Formation and Stirling Quartzite, southeastern California, determined by detrital zircon geochronology and Nd isotope geochemistry: Precambrian Research, v. 206–207, p. 182–199, doi:10.1016/j.precamres.2012.02.017.

Schrag, D.P., Higgins, J.A., Macdonald, F.A., and Johnston, D.T., 2013, Authigenic carbonate and the history of the global carbon cycle.: Science, v. 339, p. 540–543, doi:10.1126/science.1229578.

Shields, G.A., Mills, B.J.W., Zhu, M., Raub, T.D., Daines, S.J., and Lenton, T.M., 2019, Unique Neoproterozoic carbon isotope excursions sustained by coupled evaporite dissolution and pyrite burial: Nature Geoscience, v. 12, p. 823–827, doi:10.1038/s41561-019-0434-3.

Slama, J., and Kosler, J., 2012, Effects of sampling and mineral separation on accuracy of detrital zircon studies: Geochemistry, Geophysics, Geosystems, v. 13, p. 1–17, doi:10.1029/2012GC004106.

Slingerland, R., 1984, Role of hydraulic sorting in the origin of fluvial placers: Journal of Sedimentary Petrology, v. 54, p. 137–150, doi:10.1306/212F83C8-2B24-11D7-8648000102C1865D.

Slingerland, R.L., 1977, The Effects of Entrainment on the Hydraulic Equivalence Relationships of Light and Heavy Minerals in Sands: SEPM Journal of Sedimentary Research, v. Vol. 47, p. 753–770, doi:10.1306/212f7243-2b24-11d7-8648000102c1865d.

Slingerland, R., and Smith, N.D., 1986, Occurrence and formation of water-laid placers: Annual Review of Earth and Planetary Sciences, v. 14, p. 113–147.

Smith, N.D., and Beukes, N.J., 1983, Bar to bank flow convergence zones: a contribution to the origin of alluvial placers: Economic Geology, v. 78, p. 1342–1349, doi:10.2113/gsecongeo.78.7.1342.

Smith, E.F., Nelson, L.L., Tweedt, S.M., Zeng, H., and Workman, J.B., 2017, A cosmopolitan late Ediacaran biotic assemblage : new fossils from Nevada and Namibia support a global biostratigraphic link:

Smithson, F., 1950, The mineralogy of arenaceous deposits: Science Progress, v. 149, p. 10–21.

Spencer, C.J., Kirkland, C.L., and Roberts, N.M.W., 2018, Implications of erosion and bedrock composition on zircon fertility: Examples from South America and Western Australia:

Terra Nova, v. 30, p. 289–295, doi:10.1111/ter.12338.

Steidtmann, J.A., and Haywood, H.C., 1982, Settling velocities of quartz and tourmaline in eolian sandstone strata.: Journal of Sedimentary Petrology, v. 52, p. 395–399, doi:10.1306/212f7f63-2b24-11d7-8648000102c1865d.

Stevens, T., Palk, C., Carter, A., Lu, H., and Clift, P.D., 2010, Assessing the provenance of loess and desert sediments in northern China using U-Pb dating and morphology of detrital zircons: Bulletin of the Geological Society of America, v. 122, p. 1331–1344, doi:10.1130/B30102.1.

Stewart, J.H., 1970, Upper Precambrian and Lower Cambrian Strata in the Southern Great Basin California and Nevada:

Stewart, J.H., Gehrels, G.E., Barth, A.P., Link, P.K., Christie-Blick, N., and Wrucke, C.T., 2001, Detrital zircon provenance of Mesoproterozoic to Cambrian arenites in the Western United States and Northwestern Mexico: Bulletin of the Geological Society of America, v. 113, p. 1343–1356, doi:10.1130/0016-7606(2001)113<1343:DZPOMT>2.0.CO;2.

Stewart, J.H., and Poole, F.G., 1974, Lower Paleozoic and uppermost Precambrian Cordilleran Miogeocline, Great Basin, Western United States, *in* Tectonics and Sedimentation Special Publication 22,.

Summa, C.L., 1993, Sedimentologic, stratigraphic, and tectonic controls of a mixed carbonate-siliciclastic succession: Neoproterozoic Johnnie formation, southeast California: Massachusetts Institute of Technology, 616 p.

Sumner, D.Y., and Grotzinger, J.P., 2000, Late Archean Aragonite Precipitation: Petrography, Facies Associations, and Environmental Significance: SEPM Special Publication 67: Carbonate Sedimentation and Diagenesis in the Evolving Precambrian World, v. 67, p. 123–144, doi:10.2110/pec.00.67.0123.

Sumner, D.Y., and Grotzinger, J.P., 1996, Were kinetics of Archean calcium carbonate precipitation related to oxygen concentration? Geology, v. 24, p. 119–122, doi:10.1130/0091-7613(1996)024<0119:WKOACC>2.3.CO;2.

Trower, E.J., and Grotzinger, J.P., 2010, Sedimentology, diagenesis, and stratigraphic occurrence of giant ooids in the Ediacaran Rainstorm Member, Johnnie Formation, Death Valley region, California: Precambrian Research, v. 180, p. 113–124, doi:10.1016/j.precamres.2010.03.007.

Troxel, B.W., Cooper, J.D., and Wright, L.A., 1982, Basin facies (Ibex Formation) of the Noonday Dolomite, southern Saddle Peak Hills, southern Death Valley, California., *in* Geology of Selected Areas in the San Bernardino Mountains, Western Mojave Desert, and Southern Great Basin, California, Shoshone, California.

Verdel, C., Wernicke, B.P., and Bowring, S.A., 2011, The Shuram and subsequent Ediacaran carbon isotope excursions from southwest Laurentia, and implications for environmental stability during the metazoan radiation: Bulletin of the Geological Society of America, v. 123, p. 1539–1559, doi:10.1130/B30184.1.

Williams, E.G., Wright, L.A., and Troxel, B.W., 1974, The Noonday Dolomite and equivalent stratigraphic units, southern Death Valley region, California., *in* Guidebook: Death Valley Region, California and Nevada, Chicago, p. 73–77.

Witkosky, R., and Wernicke, B.P., 2018, Subsidence history of the Ediacaran Johnnie Formation and related strata of southwest Laurentia: Implications for the age and duration of the Shuram isotopic excursion and animal evolution: Geosphere, v. 14, p. 2245–2276, doi:10.1130/GES01678.1.

Wood, R.A. et al., 2015, Dynamic redox conditions control late Ediacaran metazoan ecosystems in the Nama Group, Namibia: Precambrian Research, v. 261, p. 252–271, doi:10.1016/j.precamres.2015.02.004.

Woolsey, J.R., Henry, V.J., and Hunt, J.L., 1975, Backshore Heavy-mineral Concentration on Sapelo Island, Georgia: SEPM Journal of Sedimentary Research, v. Vol. 45, p. 280–284, doi:10.1306/212f6d39-2b24-11d7-8648000102c1865d.

Wright, L.A., Williams, E.G., and Troxel, B.W., 1984, Appendix II. Type section of the newly named Proterozoic Ibex Formation, the basinal equivalent of the Noonday Dolomite, Death Valley region, California: California Division of Mines and Geology Map Sheet 34, p.:

Xiao, S., Narbonne, G.M., Zhou, C., Laflamme, M., Grazhdankin, D. V., Moczydlowska-Vidal, M., and Cui, H., 2016, Towards an Ediacaran Time Scale: Problems, Protocols, and Prospects: Episodes, v. 39, p. 540, doi:10.18814/epiiugs/2016/v39i4/103886.

Yang, S., Zhang, F., and Wang, Z., 2012, Grain size distribution and age population of detrital zircons from the Changjiang (Yangtze) River system, China: Chemical Geology, v. 296–297, p. 26–38, doi:10.1016/j.chemgeo.2011.12.016.

Zhang, F. et al., 2019, Global marine redox changes drove the rise and fall of the Ediacara biota: Geobiology, doi:10.1111/gbi.12359.

Zhu, M., Zhang, J., and Yang, A., 2007, Integrated Ediacaran (Sinian) chronostratigraphy of South China: Palaeogeography, Palaeoclimatology, Palaeoecology, v. 254, p. 7–61, doi:10.1016/j.palaeo.2007.03.025.

Figures and Figure Captions

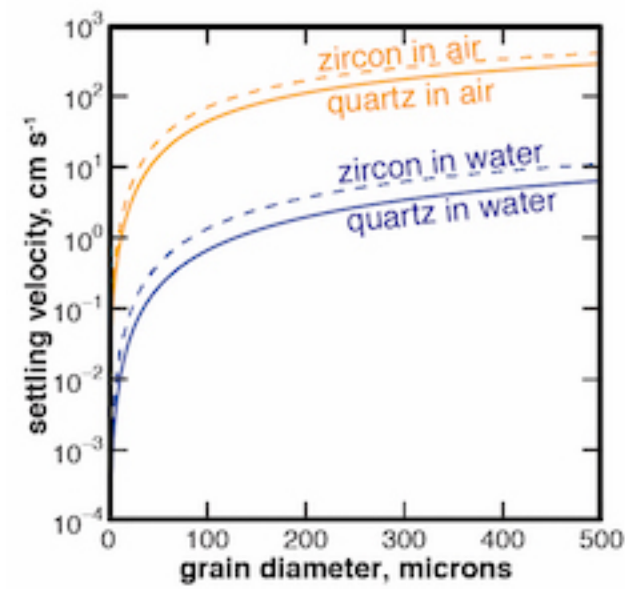

Figure 1. The settling velocities of quartz and zircon grains in water and air are shown as a function of grain diameter based on empirical measurements (Dietrich 1982, Bagheri and Bonadonna 2016, Raffaele et al. 2020). Due to its greater density, zircon grains settle more rapidly than quartz grains of the same size, so zircon grains with the same settling velocity as quartz grains are smaller. The settling velocities of quartz and zircon grains in air are more rapid because air is less viscous and dense than water. Relative to the same quartz grain size, the hydrodynamically equivalent zircon in air will be larger than the hydrodynamically equivalent zircon in water.

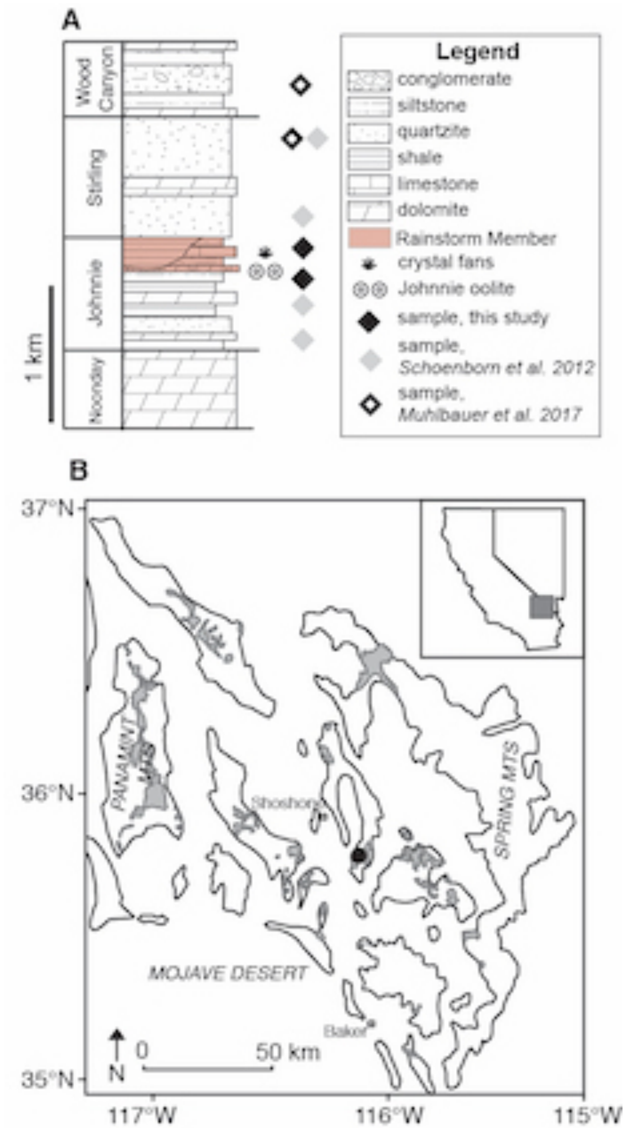

Figure 2. A. The Edicaran to Terreneuvian succession of Death Valley, Nevada and California, USA, is shown. The lowermost Noonday Dolomite is considered earliest Ediacaran near its base (Prave 1999, Petterson et al. 2015) and the Wood Canyon Formation straddles the Ediacaran-Cambrian boundary (Corsetti and Hagadorn 2000). The approximate stratigraphic position of samples from this study and previous studies (Schoenborn et al. 2012, Muhlbauer et al. 2017) are shown as diamonds. The Rainstorm Member, the particular focus of this study, is highlighted in pink.

B. The aeral extent of the Johnnie Formation, of which the Rainstorm Member is the uppermost unit, is shown in gray. The Southern Nopah Range, where Rainstorm samples were collected for this study, is marked with a black dot. Modified after Bergmann et al. 2011, figure 2.

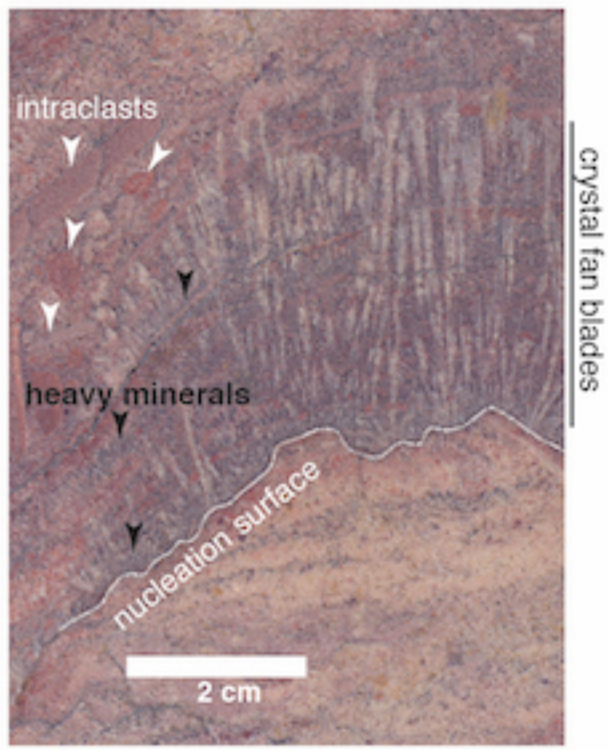

Figure 3. A representative crystal fan-bearing limestone bed from the Rainstorm Member is shown in a cut and polished slab. Formerly aragonite (Pruss et al. 2008) crystal fans nucleate on a scoured seafloor surface, traced with a dotted white line. Heavy mineral-enriched clastic detritus is abundant in the sample, visible as dark gray to black zones; a few examples are indicated with black arrowheads. Carbonate intraclasts are also abundant, and a few examples are indicated with white arrowheads. Modified after Bergmann et al. 2013, Figure 5A.

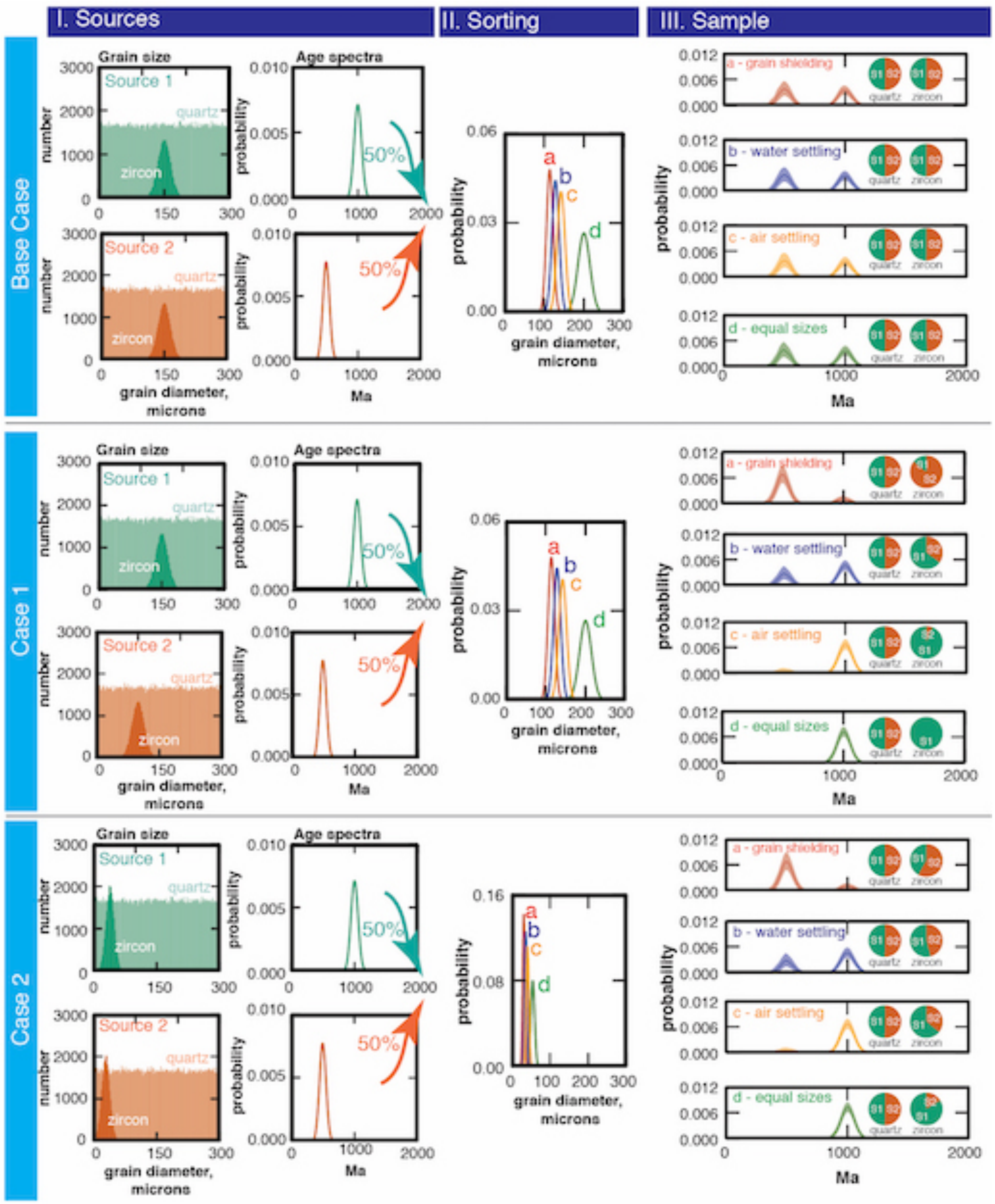
I. Sources
II. Sorting
III. Sample
Base Case
Case 1
Case 2
Grain size
Age spectra
Source 1
Source 2
quartz
zircon
number
probability
50%
grain diameter, microns
Ma
a
b
c
d
a - grain shielding
b - water settling
c - air settling
d - equal sizes
S1
S2
quartz
zircon

Figure 4. The process-dependent, hydrodynamic sorting of different zircon populations in an idealized sedimentary system is illustrated here in three cases. The grain size and age spectra of two source populations, and the proportion in which these populations are mixed, are shown in column I. Column II shows four different depositional sizes informed by four different size-density relationships between deposited quartz and zircon, from the "grain shielding" case in which deposited zircon grains are smaller than predicted by settling relationships, to the "equal sizes" case in which zircon and quartz grains have the same size. Size-density relationships from the settling of sediment in water and air are intermediate to these two cases. The resulting synthetic age spectra are shown in column III (95% confidence interval envelope), along with the proportions of grains from different sources.

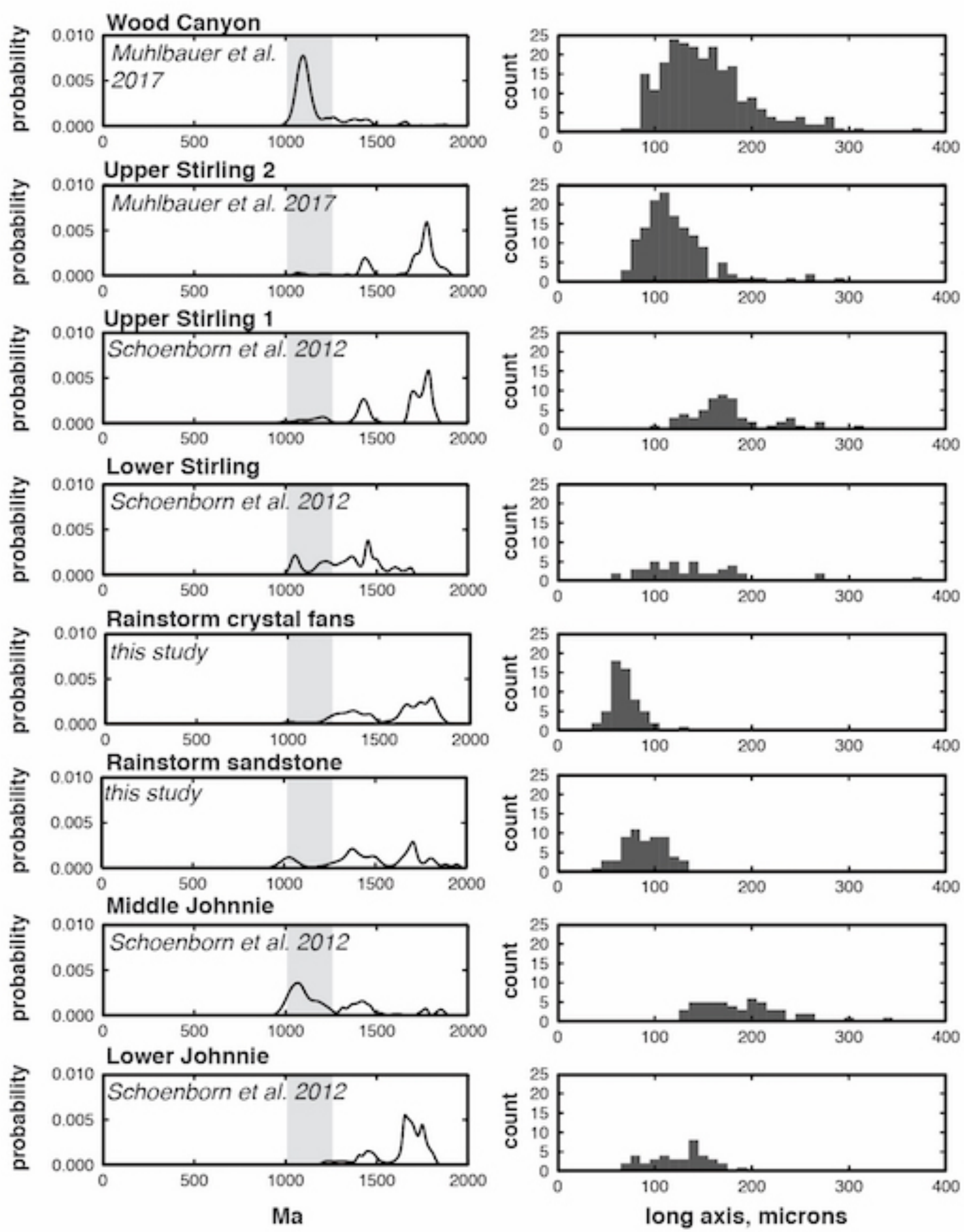

Wood Canyon
Muhlbauer et al. 2017
Upper Stirling 2
Muhlbauer et al. 2017
Upper Stirling 1
Schoenborn et al. 2012
Lower Stirling
Schoenborn et al. 2012
Rainstorm crystal fans
this study
Rainstorm sandstone
this study
Middle Johnnie
Schoenborn et al. 2012
Lower Johnnie
Schoenborn et al. 2012
probability
count
Ma
long axis, microns

Figure 5. Measured age spectra and size distributions for samples included in this study. Grenville age (1.0-1.2 Ga) ranges are highlighted in gray. Samples from the Rainstorm Member are finer-grained than other samples.

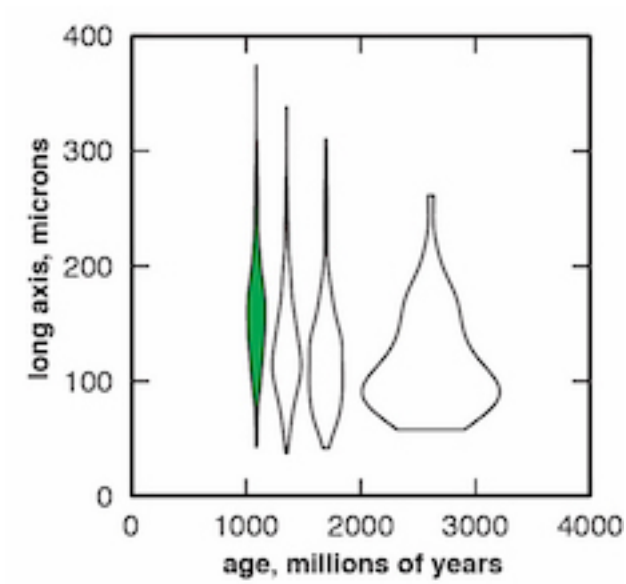

Figure 6. This violin plot describes size variation within and between age populations from detrital zircons measured by this study and others (Schoenborn et al. 2012, Muhlbauer et al. 2017). Grenville-aged grains (1.0-1.2 Ga, highlighted in green) are larger on average than their older counterparts, though all age populations contain larger and small grains.

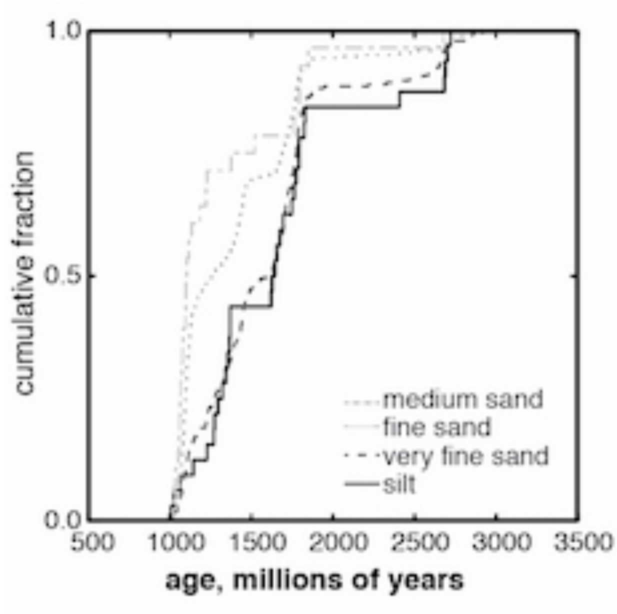

Figure 7. These empirical cumulative distribution function curves describe the fraction of grains and their ages in a detrital zircon dataset measured by this study and others (Schoenborn et al, Muhlbauer et al. 2017). The silt and very fine sand-sized grain populations are similar to ach other, as are the fine and medium-sand sized populations. The largest difference is for Grenville-aged (1.0-1.2 Ga) grains, which make up more than 50% of the fine and medium sand sized grains but less than 50% of the silt and very fine sand sized-grains.

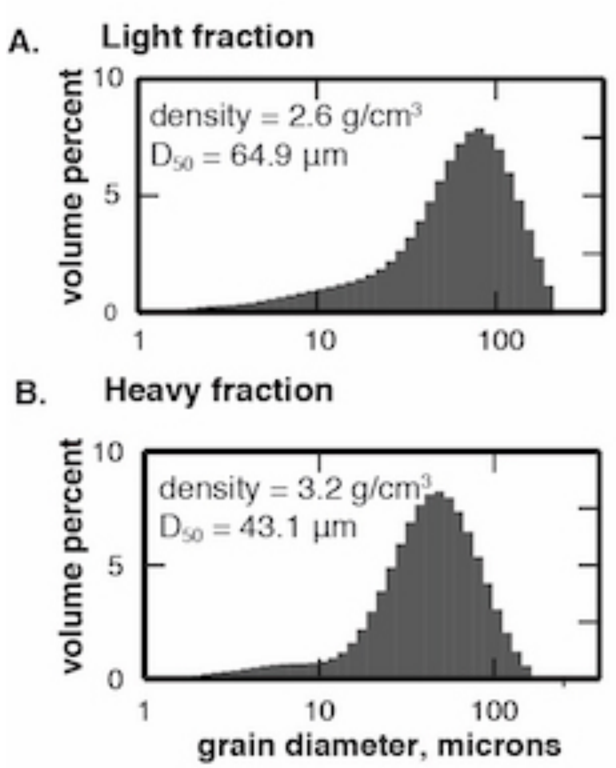

Figure 8. LPSA data for both the light and heavy fractions of crystal fan-associated detritus are shown.

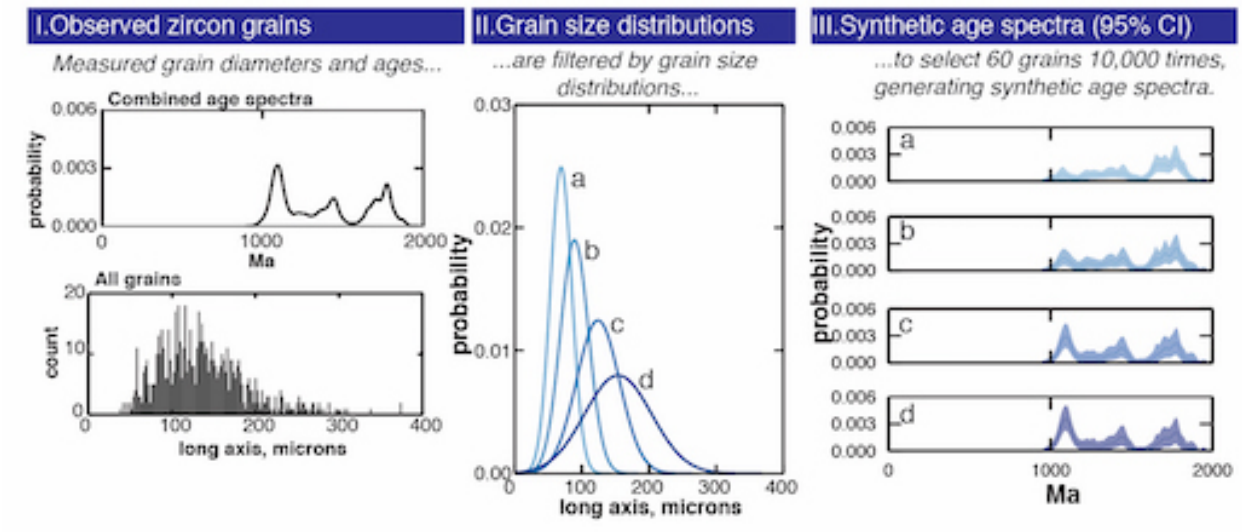

Figure 9. All measured concordant zircon grains with a known size from this study and others (Schoenborn et al, Muhlbauer et al. 2017) are shown in column I. These grains are pooled together and 60 grains are chosen 10,000 times to generate a series of synthetic age spectra. The grains are selected used size-based probability distribution functions shown in column II. The 95% confidence interval of the resulting synthetic age spectra are shown in column III. As the synthetic samples grow coarser (from a to d), the prominence of the Grenville-aged peak also grows.

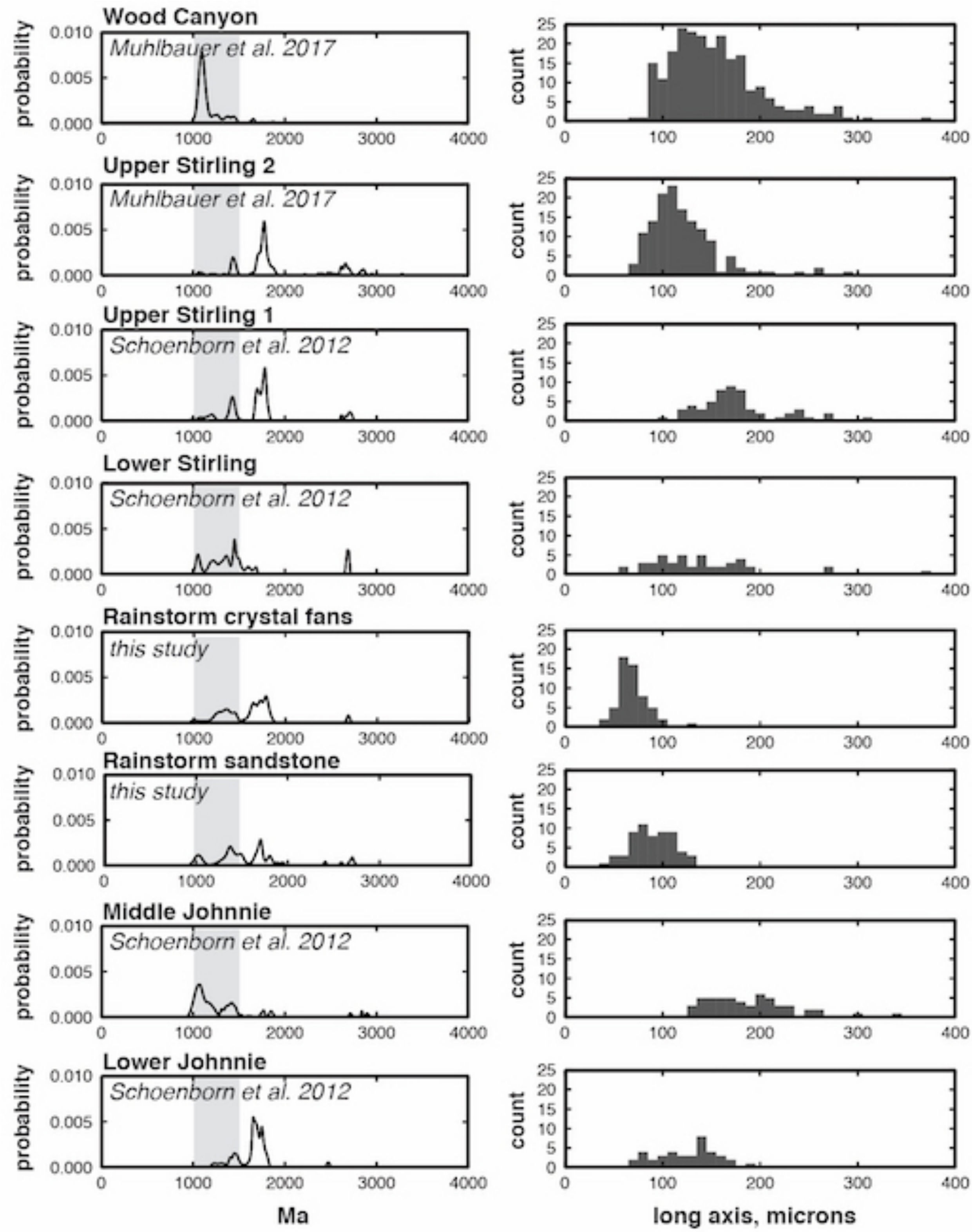

Figure S1. This figure shoes the same data as Fig. 5 in the main text but includes grains older than 2000 Ma.

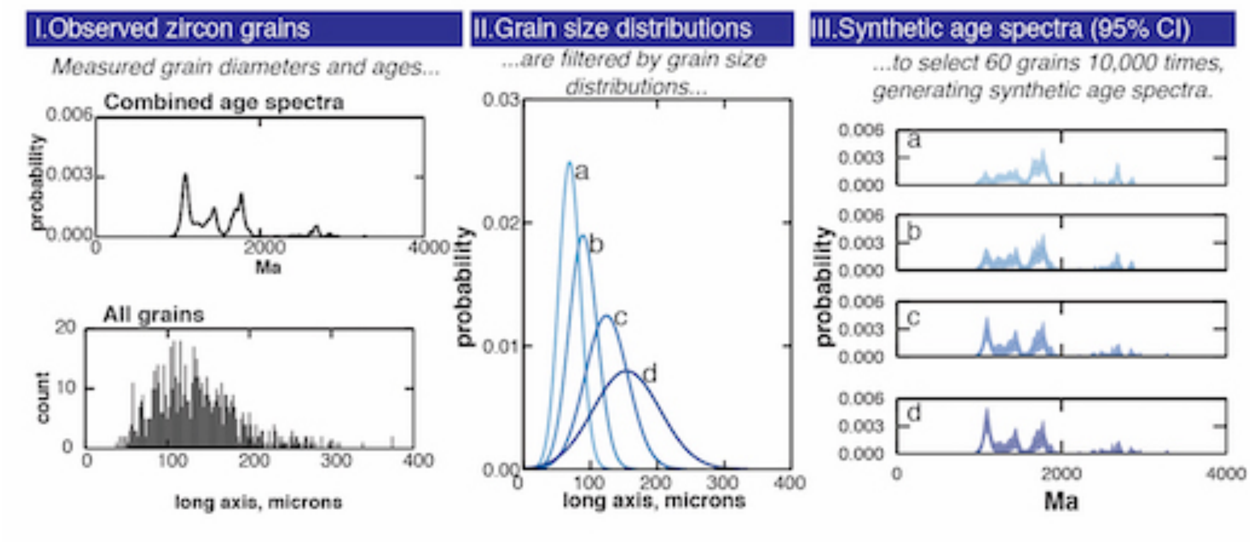

Figure S2. This figure shoes the same data as Fig. 9 in the main text but includes grains older than 2000 Ma.